Solar Energy 205 (2020) 409–431

Contents lists available at ScienceDirect

Solar Energy

journal homepage: www.elsevier.com/locate/solener

Corrosion growth of solar cells in modules after 15 years of operation

Yaowanee Sangpongsanont[a,b], Dhirayut Chenvidhya[c,*], Surawut Chuangchote[d], Krissanapong Kirtikara[c]

[a] The Joint Graduate School of Energy and Environment (JGSEE), King Mongkut's University of Technology Thonburi (KMUTT), Bangkok, Thailand
[b] Centre of Excellence on Energy Technology and Environment, Science and Technology Postgraduate Education and Research Development Office, Bangkok, Thailand
[c] CES Solar Cells Testing Center (CSSC), Pilot Plant Development and Training Institute (PDTI), King Mongkut's University of Technology Thonburi (KMUTT), Bangkok, Thailand
[d] Department of Tool and Materials Engineering, Faculty of Engineering, King Mongkut's University of Technology Thonburi (KMUTT), Bangkok, Thailand

ARTICLE INFO

Keywords:
PV modules deterioration
Annual degradation
Delamination
Corrosion on solar cells
Long-term evaluation

ABSTRACT

This paper is to study the deterioration of PV modules after 15 years of operation in Thailand. All 16 modules of a string were annually measured in the standard testing laboratory, then taken back to the same position of string since the 7th year after operation. The results and data analysis can be divided into 3 parts consisting of electrical performance evaluation, physical deterioration observation, and corrosion growth on cell ribbons. From the electrical results of performance at STC, it was found that power of modules were less than 80% of the nameplate value in the 15th year for 75% of total modules. The average degradation rates, based on nameplate, was 1.47%/year. The degradation rates of modules since the 10th year after operation were in the range of 2.5 to 3.0%. From the visual failures on the front and rear side of modules were appeared in all modules. During the 12th – 15th year, the corrosion area growth on cell ribbons, calculated by ImageJ program, was around 10–17%/3 years of ribbons area, especially for cells beside junction box. The colors of corrosion products were also observed in both color appearance and color change on each cell of selected modules. For these modules, we intend to continue operation until end-of-life of the system. Another similar module was destructed and taken to investigate. The corrosion products and color of corrosion products can be justified by EDS and referred to ASTM D130 standard. Sn and Pb corrosion products were confirmed by SEM and EDS.

1. Introduction

Cumulative PV installations, with a worldwide, increased form 14.5 MW in 2008 to 512.3 GW at the end of 2018 (IEA-PVPS, 2009; Masson and Izumi, 2019; Masson et al., 2019). In our country, Thailand, the target of PV installation is 10 GW in 2037 according to the Thailand Power Development Plan (PDP2018) and the Alternative Energy Development Plan (AEDP2015). Cumulative installation in our country was close to 3 GW at the end of 2018 (DEDE, 2019). To meet the target, the growth of installed capacity will be in magnitude of 1000 times in the period of three decades. Therefore, PV module deterioration is one of the most important of PV system reliability issue. PV module deterioration is not only affected to financial returns, but it will also be affected to environmental aspects. Therefore, there were various investigations including PV degradation rate, modules failure mechanism, long term evaluation of systems, test methods to ensure lifetime of modules, standard improvement, etc.

Regarding PV degradation, National Renewable Energy Laboratory (NREL) reported that degradation rate of PV modules which were installed and exposed on field in US, Europe, Japan and Australia. It was found that crystalline silicon (c-Si) PV modules had average degradation 0.8% / year, but they depend on the starting time of installation, PV module quality and environment area of installation (Jordan and Kurtz, 2013). The National Institute of Advanced Industrial Science and Technology (AIST) had installed PV grid-connected system in Japan latitude 32.2 N and longitude 130.3 E from 2010 to 2016 that presented the degradation rate of mono-crystalline silicon (mono-Si) PV modules was 2.6%/year and the poly-crystalline silicon (poly-Si) PV modules was 2.2%/year (Ishii and Masuda, 2017). Photovoltaic Reliability Laboratory (ASU-PRL) reported that the degradation rate of poly-Si PV Modules which were installed at hot-dry climate withstand more than 13 years is 2.29%/year (Janakeeraman et al., 2014). Some researchers reported that the 90 mono-Si PV modules which were installed more than 22 years in the composite climate of India shown the average of power degradation was 1.9%/year. However, the maximum and minimum of degradation rates were 4.4%/year and 0.3%/year

* Corresponding author.
E-mail address: dhirayut.che@kmutt.ac.th (D. Chenvidhya).

https://doi.org/10.1016/j.solener.2020.05.016
Received 7 January 2020; Received in revised form 3 May 2020; Accepted 4 May 2020
Available online 04 June 2020

Table 1
Summary of investigations of degradation rates (DR).

Ref	Period of study	Field exposure	Measurement	Degradation rates
Jordan and Kurtz, 2013	1973–2013	US, Europe, Japan and Australia	Field/Lab	c-Si high 0.8%/year median0.5%/year
Ishii and Masuda, 2017	2010–2016	Japan	Field	mono-Si 2.6%/year poly-Si 2.2%/year
Janakeeraman et al., 2014	2001–2014	US	Field	poly-Si 2.29%/ year
Rajput et al., 2016	1994–2016	India	Field	mono-Si Average 1.9%/ year Max 4.4%/ year Min 0.3%/ year
Virtuani et al., 2019	1982–2017	Europe	Lab	(22%) is 0.2%/year (73%) is 0.7%/year
da Fonseca et al., 2020	2004–2019	Brazil	Lab	mono-Si 0.7%/year
Limmanee et al., 2016	2013–2016	Thailand	Lab	c-Si 0.5%/year
Sangpongsanont et al., 2013, 2016	2003–2016	Thailand	Lab	mono-Si 1.14%/ year poly-Si 1.41%/year

Table 2
The summary of corrosion effect on PV modules is shown in Table 2.

Ref	Measurement	corrosion
Kraft et al., 2015	– aging (damp heat)/Lab – scanning electron microscope (SEM) – the corrosion of the glass layer	– corrosion mechanism induced by acetic acid – corrosion products of the contact (lead, silver) by chemical trace
Kim et al., 2016	– aging (damp heat)/Lab (85 °C, 85% RH, 4000 h)	– degradation of the PV modules occurred by the aging effects – the increasing of series and contact resistance of metal components by silicon and silver finger corrosion
Ferrara and Philipp, 2012	– Field/Lab (hot-spot, mechanical load, humidity-freeze, damp-heat, thermal cycling/STC)	-corrosion occurred on connection materials- corrosion detected by visual observation-corrosion effect on electrical characteristic of PV modules (increasing of series resistance)-gases can cause corrosion as being acid HNO_3, HCL, H_2SO_4 etc
Xiong et al., 2017	– -Aging /Lab (25 °C, 45%RH, 2 months) (25 °C, 85%RH, 240 h) (25 °C, 55%RH, 240 months, acetic acid)	– corrosion behavior of rear electrode in cells is presented yellow and indigo – corrosion occurs at the soldered connection – corrosion region will expand from the edge to the center between Ag electrode and Sn37Pb alloy – -metals with lower potential values would be corroded first
Li et al., 2018	– Aging/Lab (85 °C, 85%RH, damp heat 1000 h) (85 °C, 85%RH, bias −1000 V 300 h)	– corrosion of materials in solar cells occurs on their corrosion resistance to the alkaline solution – corrosion and delamination are interactive and promote the formation and propagation of one another

(a) APV grid-connected system

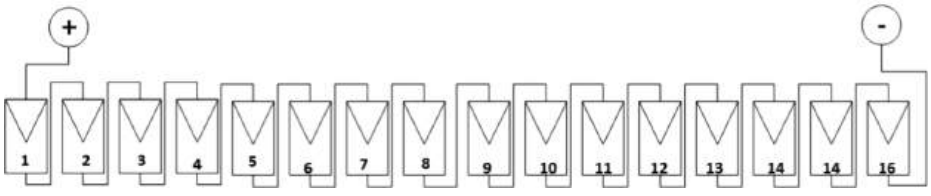

(b) PV modules configuration

Fig. 1. A PV system and PV modules configuration of the selected string.

Table 3
List of Instrument.

Test item	Instrument
Measurement of performance at STC	Pasan solar simulator IIIb with class AAA
Visual observation	Canon – EOS77
Insulation test	Hipot test: Chroma 19052
Electroluminescence	EL camera: Buchanan EL-MES CAM1
	DC power supply: Agilent N5769A 87J

respectively (Rajput et al., 2016). The oldest PV system installation in Europe presented the average degradation rate after 35 years operation into 2 groups one, 22% of number of samples, is 0.2%/year another, 70% of number of samples, is 0.69%/year (Virtuani et al., 2019). In Brazil, the average of degradation rate of monocrystalline Si PV modules was 0.70%/year for the PV system after 15 years operation. Visual defects, consisting of browning, coating oxidation, milky pattern, cell cracks, backsheet delamination, by-pass diode defect and hot spots, were found (da Fonseca et al., 2020). In Thailand, the National Science and Technology Development Agency (NSTDA) presented about poly-Si modules which were installed in hot and humid climate the degradation rate is 0.5%/year (Limmanee et al., 2016). In our previous works reported the degradation rate of mono-Si and poly-Si modules which were installed near the gulf of Thailand were 1.14%/year and 1.41%/year (Sangpongsanont et al., 2013, 2016). The summary of investigations of degradation rates are shown in Table 1.

There were some researches to study causes of PV modules degradation, in different kind of installation environments, consisting of discoloration, browning, yellowing on encapsulant materials ((Mani)GovidaSamy TamizhMani, 2013; Ferrara and Philipp, 2012). After Ethyl Vinyl Acetate (EVA) was exposing by UV irradiation, high temperature and humidity, chemical structure are change and formation of water and acetic acid (Gagliardi et al., 2017). These effects led to EVA degradation which can observe on EVA discoloration. Browning EVA results in transmittance of photon from solar irradiance to PV cell that made direct effect to short circuit current (Isc) and maximum power (Pm) of PV module (BBW, 2003). Browning was not only present on superstrate but also on substrate. Backsheet use for protecting modules from UV, moisture, high temperature, wind and acting as electrical insulators. Degradation of it comes from changing of chemical structure due to reflection of UV irradiance to each layer in module. Future moisture and high temperature induce browning and tear on backsheet which effect to Pm of PV modules (Jorgensen et al., 2006; Kim et al., 2016). Delamination presented on a same layer of browning that on encapsulant material. In an extended of delamination a blistering will be allow for water and gases insert into EVA/cell layer (Ferrara and Philipp, 2012). After metallic interconnection breakages, such as frames, connectors, cables, cell interconnection, ribbon, busbar and gridline then atmospheric humidity or combination with gases penetrated into encapsulant layer. That cause was led to corrosion. Moreover, higher temperature will accelerate the reaction. Corrosion is direct effect to series resistance (Rs) and Pm. Corrosion mechanisms are occurred on ribbon and gridline because of water and acetic acid from EVA degradation. Soldered connections in cells were dissolving in water and reaction like galvanic corrosion or acid corrosion. The lowest potential electrode energy of metal was going to corrode first (Kraft et al., 2015; Xiong et al., 2017). Correlation of corrosion and delamination were interactive and promote the formation and propagation of one another (Li et al., 2018). The summary of corrosion effects on PV modules are shown in Table 2.

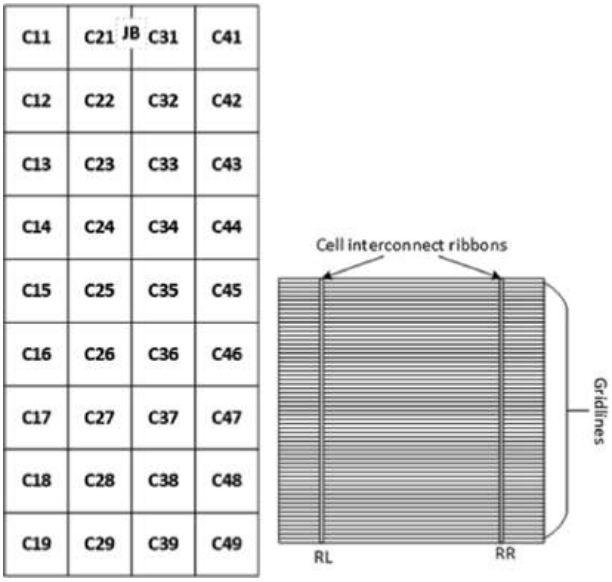

Fig. 3. Cell layout on module and code of cell interconnect ribbons.

This paper aims to investigate the metallic corrosion growth in PV modules put into operation more than 15 consecutive years. At the beginning of the PV system installation, there were an ambitious project, Solar Home Systems (SHS), in Thailand. All 16 PV modules, one whole string, were taken to measure in the standard testing laboratory and taken back to install at the same positions in every year. The PV system monitoring was well equipped since the 7th year after beginning. By the systematic study, we expect to observe the growth of deterioration, especially metallic corrosion growth on cell ribbons in this investigation. The main contribution of this paper consists of the growth of corrosion of metallic ribbon on solar cells, and degradation rates. All PV modules in a series string were taken back to measurement at the standard testing laboratory in every year. We did not find the investigation mentioned long term evaluation by taken back whole modules in a series string to measure in the testing laboratory every year. Most of investigation performed the measurement at the beginning of systems and then measured at the end of life or at the n^{th} year. Therefore, we have the measurement results of PV module during the period of PV system lifetime. We can evaluate the progress or growth of deterioration such as metal corrosion growth in this paper.

2. Methodology

This work focuses on the deterioration of PV modules in the field exposure conditions more than 15 consecutive years in Thailand. All modules under investigation were annually taken back to the standard testing laboratory. The observation of corrosion growth was highlighted.

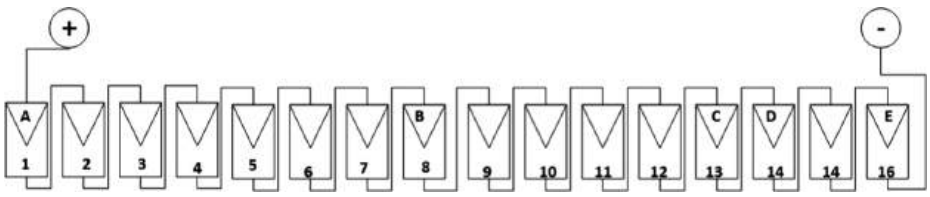

Fig. 2. the 5 selected modules (Module A, B, C, D and E).

Table 4
Electrical parameters obtained by measurement of performance at standard test condition (STC).

	Year	Module No.															
		1	2	3	4	5	6	7	8	9	10	11	12	13	14	15	16
Power at STC (Wp)	7th	111.4	112.3	113.4	112.7	113.1	113.9	112.0	114.2	112.5	113.8	111.7	111.8	111.7	113.4	111.0	108.7
	9th	106.8	108.3	110.2	110.1	110.2	109.6	108.2	108.5	109.0	108.8	109.6	106.2	103.8	109.2	105.5	104.2
	10th	103.4	105.6	108.6	107.9	108.4	107.7	104.9	107.4	108.0	105.8	105.9	104.0	104.2	108.0	101.6	103.5
	11th	100.8	102.6	106.4	106.3	106.7	105.6	104.7	106.8	108.0	105.0	103.0	101.5	103.5	106.0	102.7	101.7
	12th	98.9	100.4	104.6	103.6	103.8	103.3	103.0	104.9	104.2	102.4	98.2	99.0	97.2	102.9	100.0	100.9
	13th	97.2	97.5	101.3	101.2	101.1	100.8	101.6	103.3	101.7	99.6	97.9	95.1	93.1	100.4	98.8	97.9
	14th	93.5	93.7	97.0	98.7	99.2	97.3	99.3	100.7	100.0	93.4	96.1	92.9	92.6	95.1	95.8	96.1
	15th	90.4	90.0	93.7	96.1	97.3	94.7	97.3	98.4	95.2	92.8	93.4	90.9	86.5	92.7	93.3	94.3
Short circuit current (A)	7th	7.33	7.45	7.43	7.29	7.34	7.47	7.46	7.41	7.52	7.46	7.43	7.48	7.40	7.44	7.36	7.34
	9th	7.25	7.39	7.39	7.32	7.32	7.44	7.45	7.35	7.43	7.36	7.42	7.40	7.33	7.37	7.29	7.33
	10th	7.19	7.32	7.32	7.18	7.25	7.38	7.29	7.28	7.38	7.30	7.35	7.34	7.27	7.30	7.16	7.21
	11th	7.14	7.28	7.29	7.14	7.21	7.35	7.27	7.24	7.35	7.25	7.31	7.29	7.22	7.26	7.11	7.18
	12th	7.11	7.27	7.25	7.10	7.19	7.31	7.25	7.22	7.29	7.24	7.21	7.26	7.12	7.21	7.10	7.20
	13th	7.09	7.21	7.18	7.06	7.17	7.30	7.23	7.20	7.26	7.17	7.19	7.24	7.07	7.17	7.08	7.17
	14th	7.08	7.23	7.18	7.03	7.18	7.29	7.23	7.23	7.26	7.19	7.16	7.23	7.05	7.17	7.09	7.19
	15th	7.01	7.18	7.14	7.00	7.18	7.25	7.21	7.20	7.22	7.17	7.16	7.17	7.02	7.16	7.06	7.20
Open circuit voltage (V)	7th	21.7	21.8	21.8	21.7	21.8	21.8	21.8	21.8	21.8	21.8	21.8	21.7	21.8	21.8	21.7	21.7
	9th	21.6	21.7	21.7	21.7	21.7	21.7	21.7	21.7	21.7	21.7	21.7	21.7	21.7	21.7	21.7	21.7
	10th	21.7	21.8	21.8	21.7	21.8	21.8	21.8	21.8	21.8	21.7	21.8	21.7	21.8	21.8	21.8	21.7
	11th	21.7	21.7	21.7	21.7	21.7	21.8	21.7	21.7	21.7	21.7	21.7	21.7	21.7	21.8	21.7	21.7
	12th	21.6	21.7	21.7	21.6	21.7	21.7	21.7	21.7	21.7	21.7	21.7	21.6	21.7	21.7	21.7	21.7
	13th	21.6	21.7	21.7	21.7	21.7	21.7	21.7	21.7	21.7	21.6	21.7	21.6	21.7	21.7	21.7	21.7
	14th	21.6	21.7	21.6	21.6	21.7	21.7	21.7	21.7	21.7	21.5	21.7	21.6	21.7	21.7	21.7	21.7
	15th	21.7	21.7	21.7	21.7	21.7	21.7	21.8	21.7	21.7	21.7	21.7	21.7	21.7	21.7	21.7	21.7

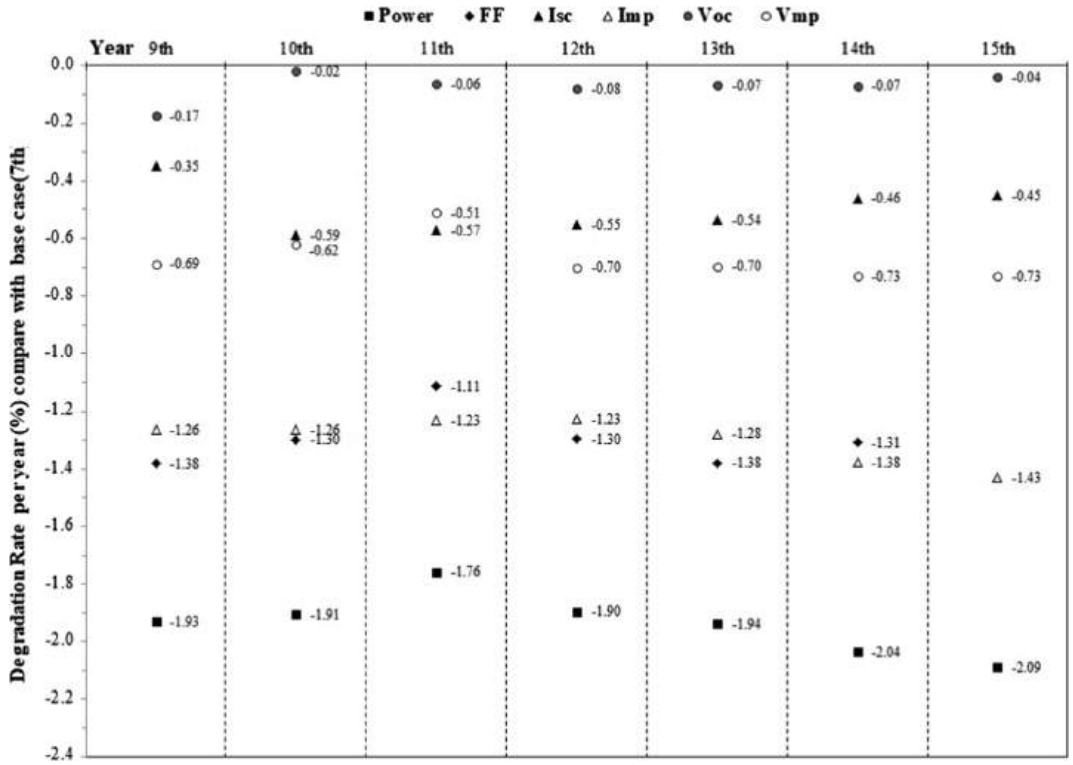

Fig. 4. The annual degradation rate of each parameter comparing with the base case (the 7th year).

2.1. Site and PV system information

One string of a PV grid-connected system was selected in this study. PV modules of the system were installed on each free-standing rack mount structure on the flat roof of a building since 2003. The site location is, at 13°34′ North latitude and 100°26′ East longitude, on the southern region of Bangkok, Thailand. From the general environmental condition of Bang Khun Thian District of Bangkok, the site lie on 1–1.5 m above sea level. The climate condition of Bangkok is Aw according to the Köppen-Geiger climate classification (https://en.climate-data.org/asia/thailand/bangkok/bangkok-6313/, 2020). The average temperature in Bangkok is 28.1 °C. About 1430 mm of precipitation falls annually. The average global solar irradiation is about 5.24 kWh/m2/day (http://www.dede.go.th/, 2017). There were 16 poly-crystalline PV modules connected in series of a string. PV modules were put into operation since 2003, while the measuring equipment were well

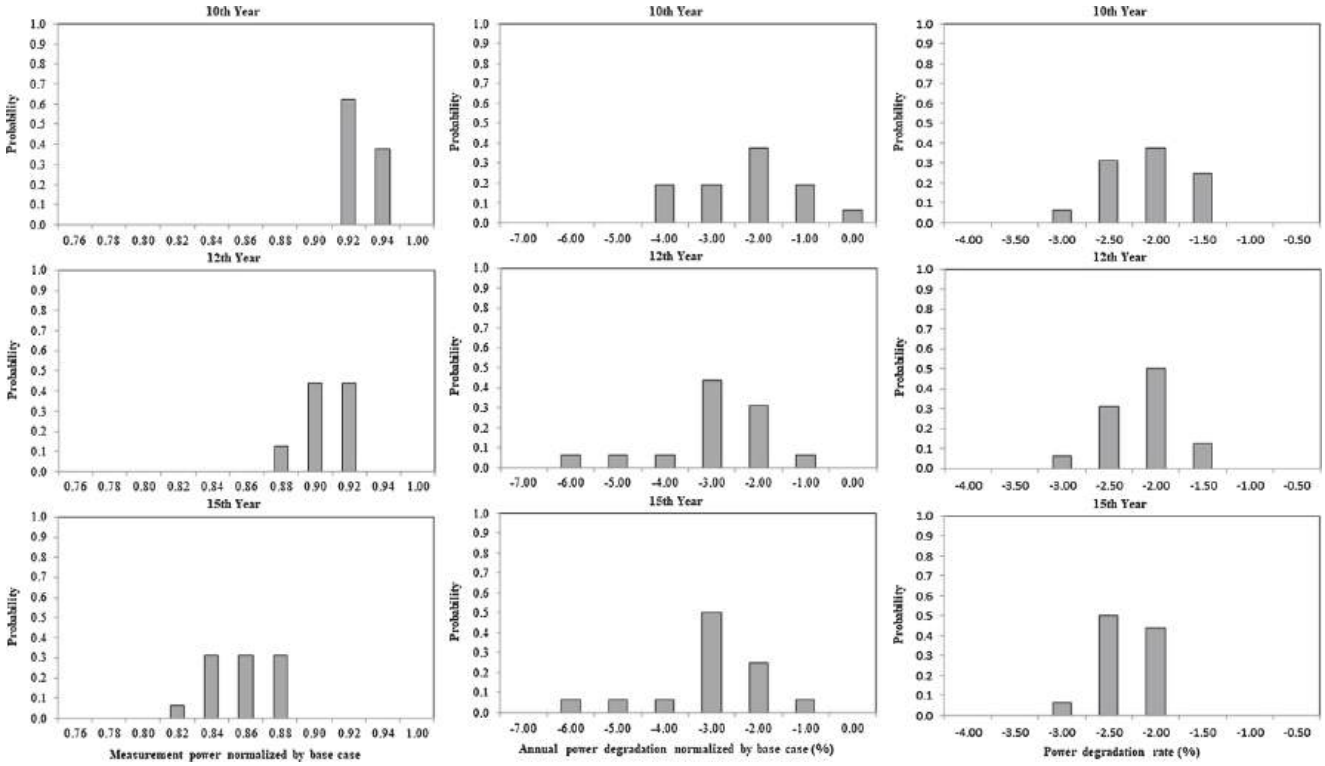

(a) Measurement power (b) Annual power degradation (c) Power degradationrate

Fig. 5. Distribution of Pm on the 10th, 12th and 15th year normalized by Pm on the base case (the 7th year).

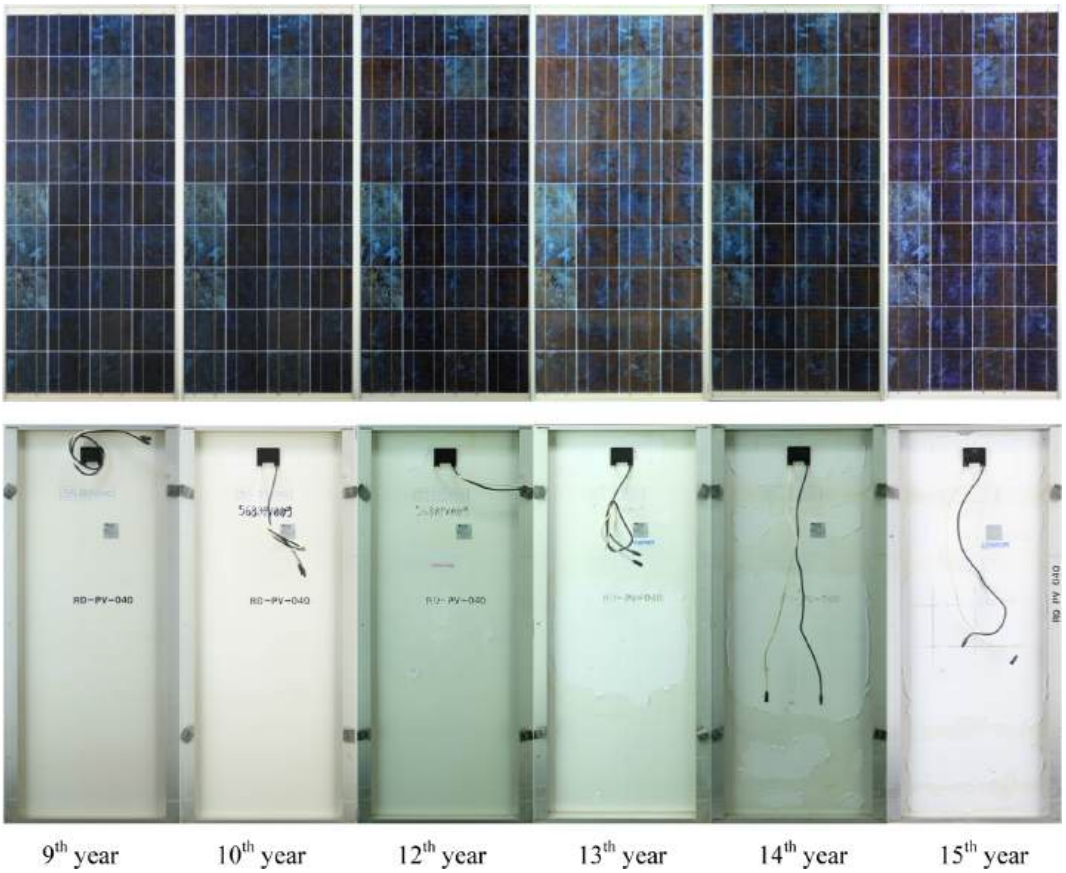

Fig. 6. Images of front side and rear side of Module No. 13 (Module C) during the 9th to the 15th year.

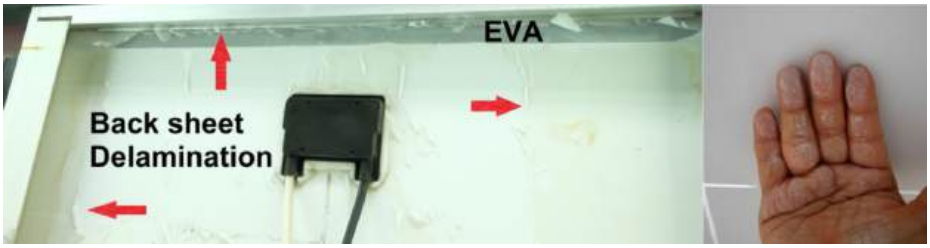

Fig. 7. Back sheet delamination and chalking.

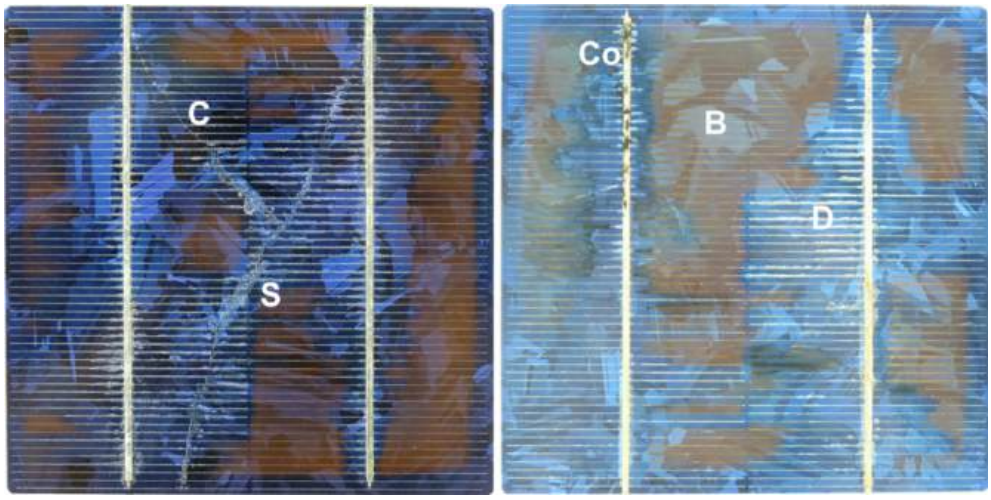

Fig. 8. Visual defects appeared on a cell such as Browning (B), Crack (C), Corrosion (Co), Delamination (D) and Snail trails (S).

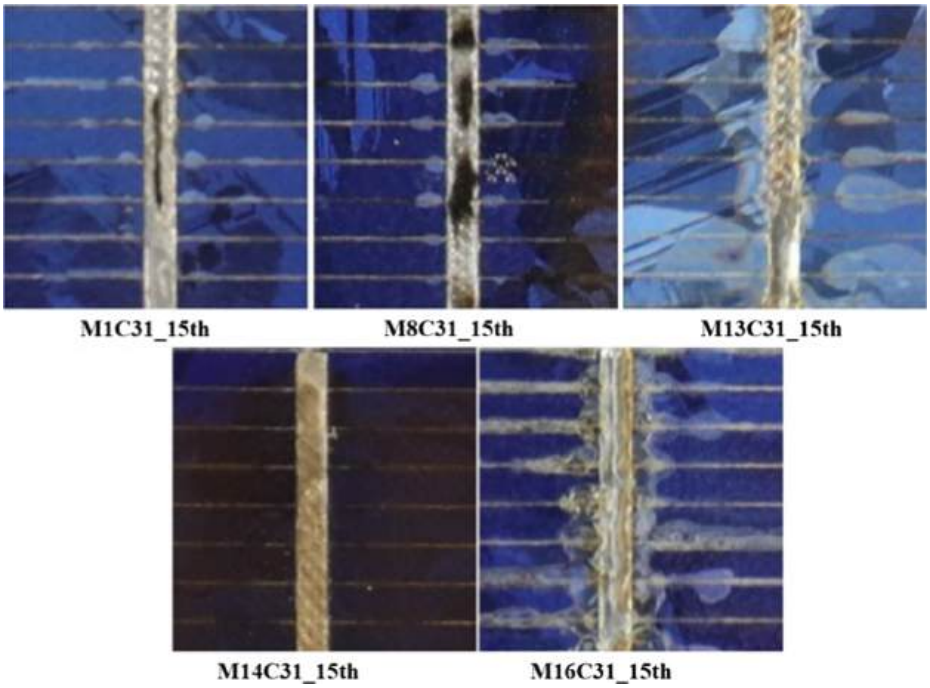

Fig. 9. Colors of corrosion on ribbon and gridline consist of yellow, light gray, dark brown and black. (For interpretation of the references to color in this figure legend, the reader is referred to the web version of this article.)

set up in 2010. The data consisting of in-plane solar irradiance, ambient temperature and humidity, wind data and module temperature, were collected in once a minute. Each PV module was fixed in its position since 2010, i.e. Module No. 1 was installed at the positive end of string, or Module No.16 was installed at the negative end of string. The photo of the system and a string configuration are shown in Fig. 1.

The specification of each PV module is poly-crystalline silicon 120 Wp, short circuit current (Isc) 7.81 A, current at maximum power (Imp) 7.02 A, open circuit voltage (Voc) 21.30 V, voltage at maximum power (Vmp) 17.10 V, and fill factor (FF) 0.72. PV modules in this study were local assembly with foreigner brand. The first year of module operation was 2003, so the 2010 is called the 7th year, and the 2018 is called the

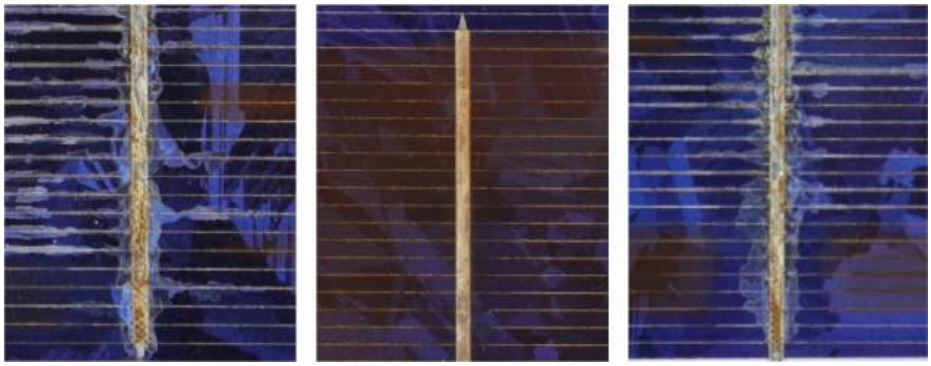

(a) M8C21_15th year (b) M13C11_15th year (c) M16C31_15th year

Fig. 10. Corrosion on ribbon (a) corrosion with delamination (b) corrosion with browning (c) corrosion with delamination and browning.

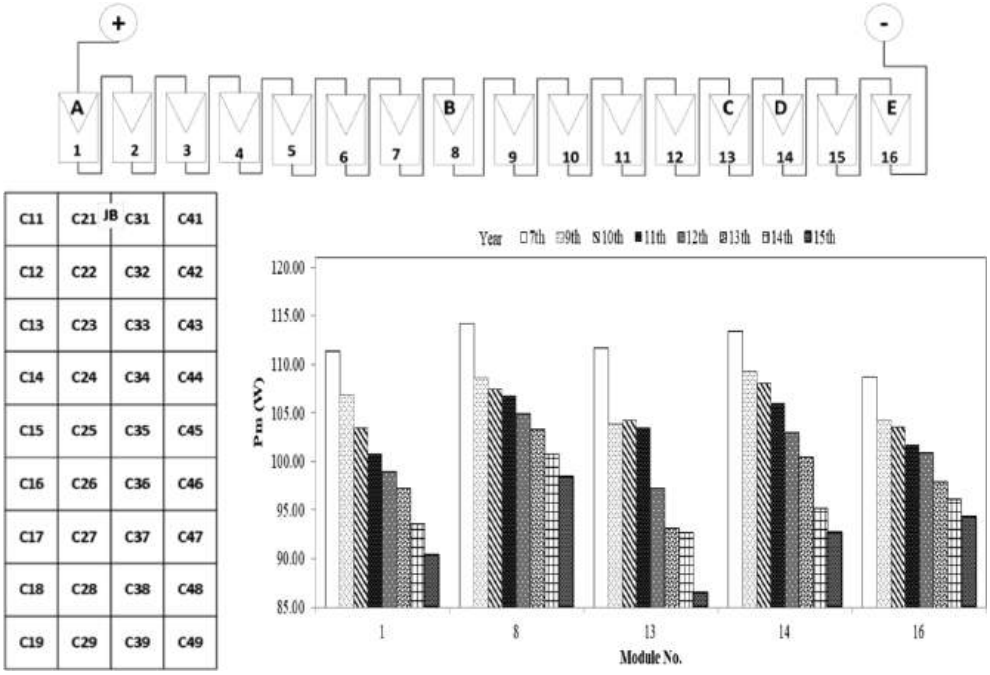

Fig. 11. the schematic and layout of the selected modules and cell layout and Pm of each selected module.

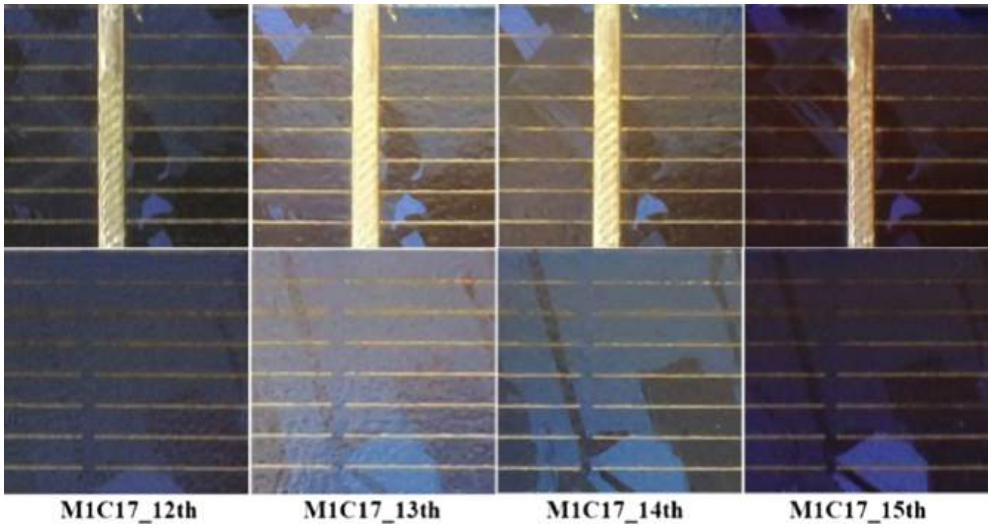

Fig. 12. Changing of corrosion colors during the 12th–15th year.

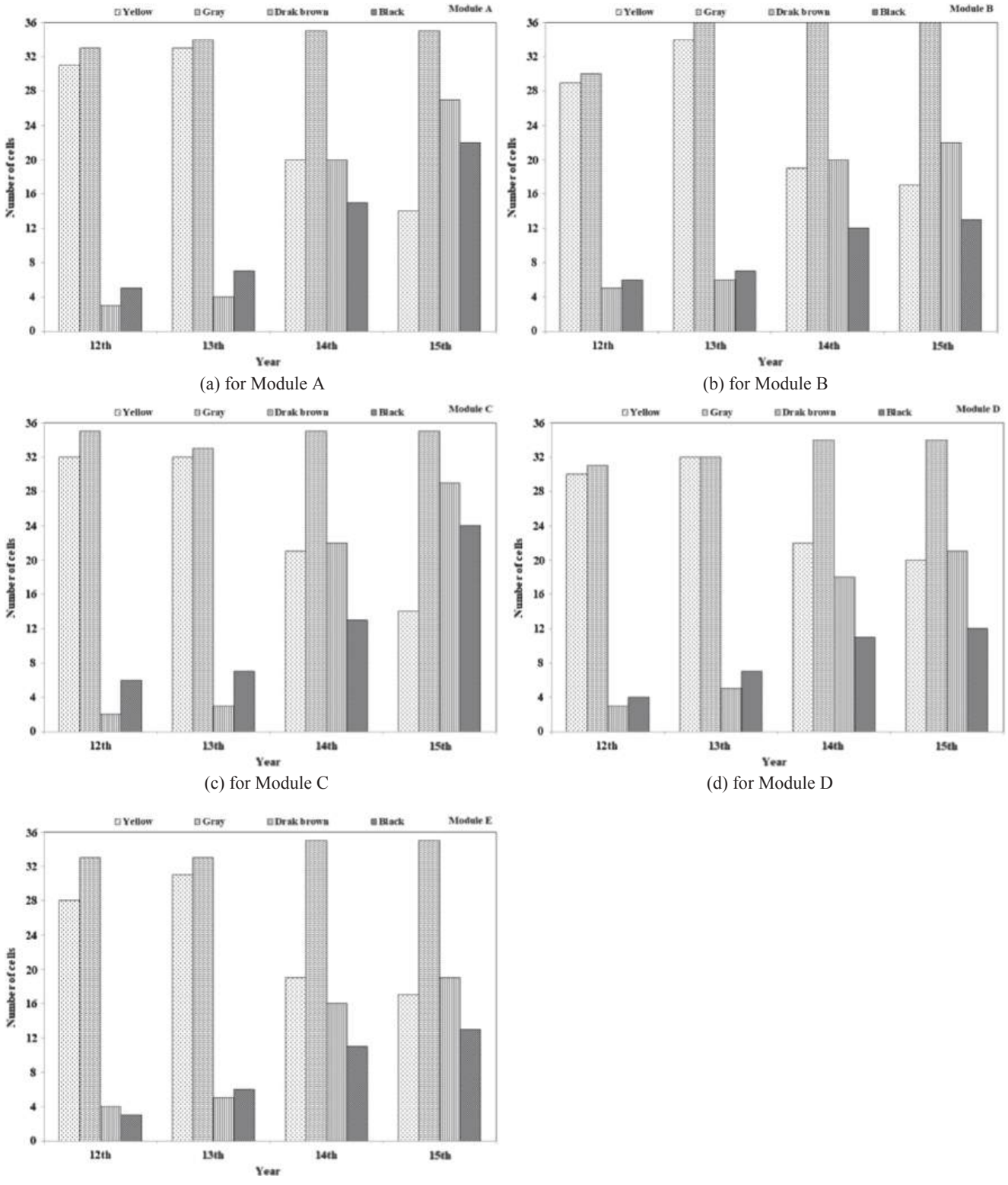

(a) for Module A

(b) for Module B

(c) for Module C

(d) for Module D

(e) for Module E

Fig. 13. Number of cells appearing each corrosion color on ribbon of each selected module.

15th year in this paper, respectively.

2.2. Measurement and evaluation of PV modules

PV modules in this string were annually measured some test items according to IEC61215:2005 since 2010. All modules were annually taken back and forth from the site to the standard testing laboratory, according to ISO/IEC17025 accreditation. The measurements, according to IEC61215:2005 clause 10.1, 10.6, 10.3 and IEC TS60904-13, were performed by the accreditation testing laboratory according to ISO/IEC17025 standard. The Test items consisted of measurement of performance at STC, Visual observation, Insulation test and

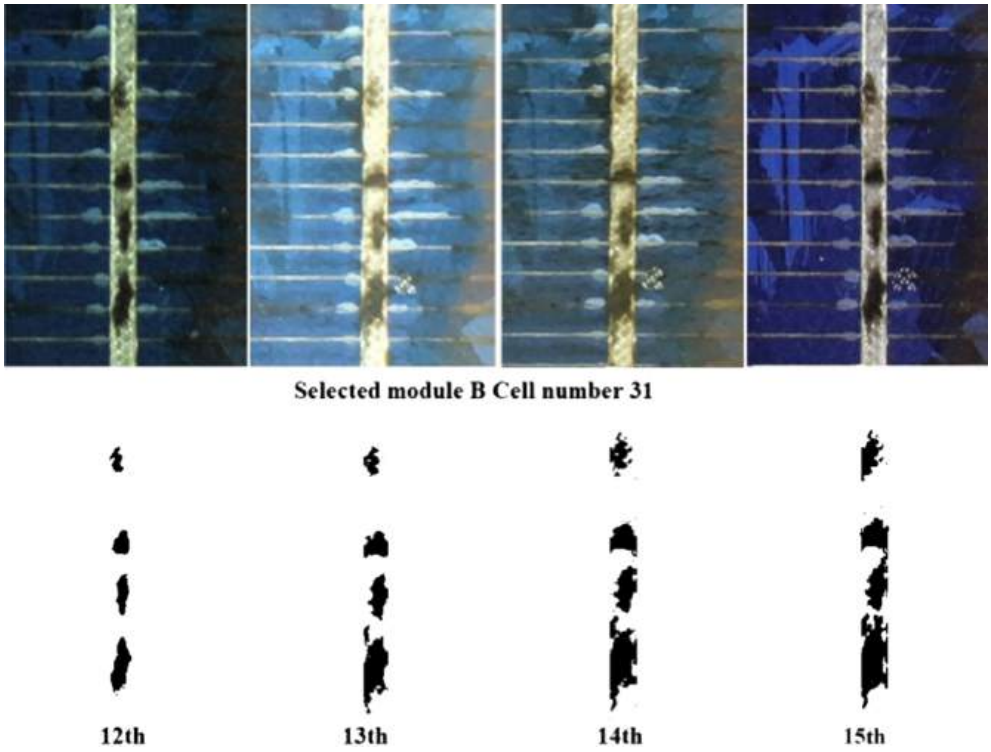

Fig. 14. Images of cell 31 of the Module: B.

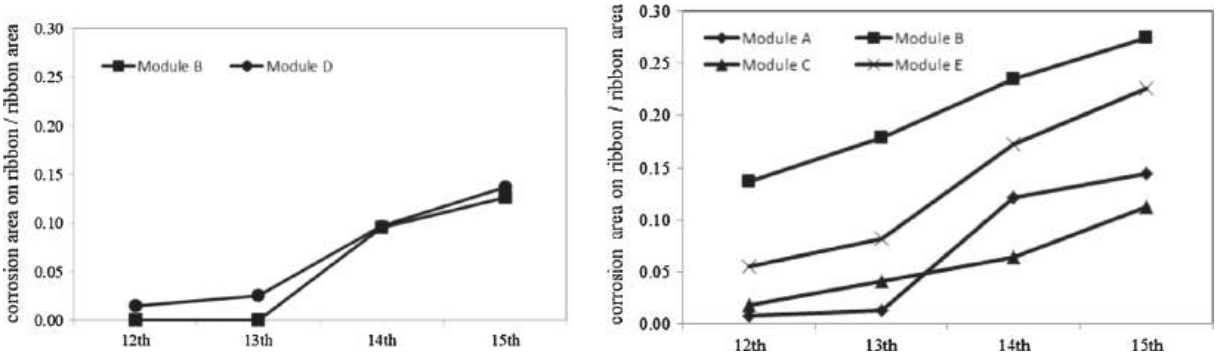

(a) for C21 cells of selected modules (b) for C31 cells of selected modules

Fig. 15. Increasing of corrosion area on both ribbons of C21 and C31 cells appeared in selected modules during the 12th–15th year.

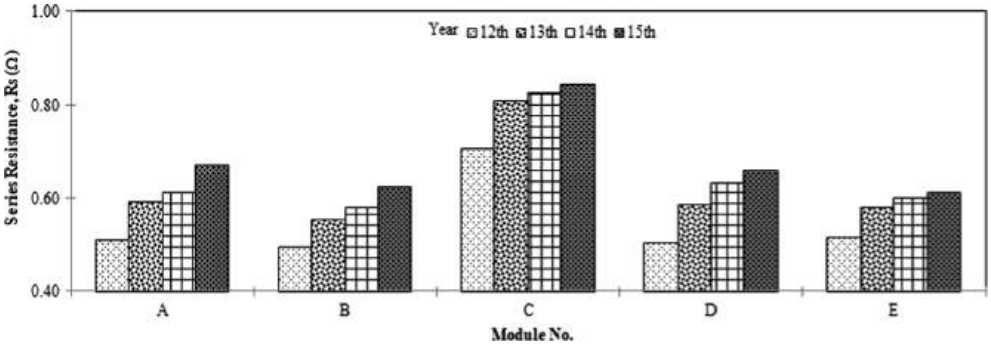

Fig. 16. Increasing series resistance of selected Modules during the 12th–15th year.

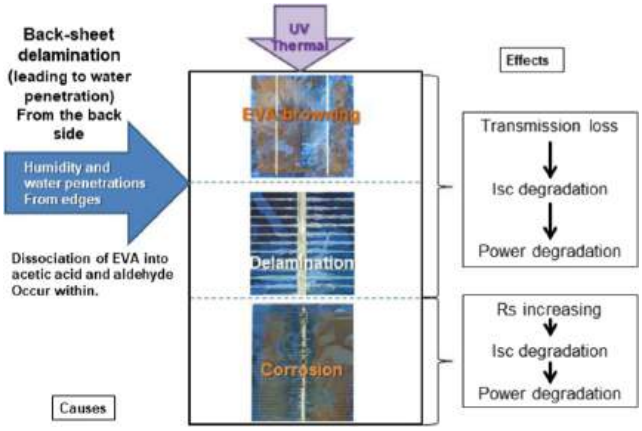

Fig. 17. Model of causes and effects of deterioration.

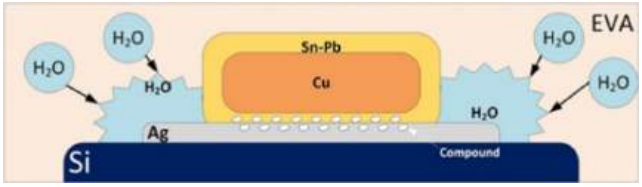

Fig. 18. Possible corrosion mechanism in a cell.

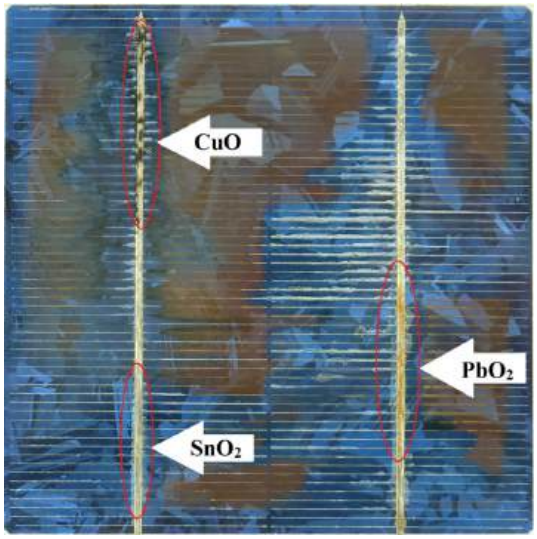

Fig. 19. Color of corrosion products of cell C31 of Module B in the 14th year.

electroluminescence. The measurement of performance at standard test condition (STC) was performed according to IEC61215:2005 clause 10.6 and IEC60904-1. The visual observation was done according to IEC61215:2005 clause 10.1 for failure inspection, and the additional observation was individually taken a photo on each cell in each module. The insulation test was done according to IEC61215:2005 clause 10.3 for checking electrical insulation withstand. Electrical parameters, consisting of current–voltage characteristic (I-V curve), short-circuit current (Isc), open-circuit voltage (Voc), current at maximum power point (Im), voltage at maximum power point (Vm), power at maximum power point (Pm), fill factor (FF), were obtained from solar simulator set in measurement of performance at STC. The uncertainty of measurement for performance at STC is 2.24%. Each module is always fixed its position as shown in Fig. 1. Test items consist of the performance measurement at standard test condition (STC), insulation test, visual inspection and Electroluminescence test (EL). The EL measurement was beginning in the 13th year. Instrument were listed as shown in Table 3.

The annual electrical degradation rates (DR) were calculated according to the equation (1)

$$\%\text{Degradation rate} = \frac{X(t_n) - X(t_0)}{X(t_0)\cdot\Delta t}\cdot 100 \quad (1)$$

where

$X(t_n)$ represents the value of the electrical parameter considered at the STC conditions respectively at time
$X(t_0)$ represents the value of the nameplate parameter, or represents the value of the parameter at the 7th year of PV system (2010)
$t_0$represents the initial time corresponding to the first installation or represents the time corresponding to the first measurement on the 7th year of PV system (2010)
t_n represents the instant of carrying out the tests
Δt represents the exposure duration in the field of the PV modules.

Parameters obtained by IV characteristics at STC condition were evaluated the annual degradation. Insulation test results were observed. Images of PV modules, taken by visual inspection test and Electroluminescence test, were compared over the time. Evaluation of modules deterioration can be done by electrical parameters in concurrent with images observation.

2.3. Investigation of corrosion growth

During the 12th–the 15th year under operation of the PV system, the metallic corrosions on each cell were observed for annually increasing of area, length and color change. The running numbers of modules, from the positive polarity end of the string to negative polarity end of the string, were called Module No.1 to Module No. 16, respectively. In practical, all modules were investigated, but we selected only 5 modules from 16 modules to show the details in this paper. The five modules, as shown in Fig. 2, consist of a module located at positive end (M1), a module located at negative end (M16), a module located at the middle of string (M8) and other two modules with maximum percentage of power degradation (M13 and M14).

There are 36 cells in series of each module. We define the code of each cell and also define the code of cell interconnection ribbons as shown in Fig. 2. A junction box of each module is located at the back side beside the two cells, C21 and C31 at the front side. The ribbon on right side is called RR, and the ribbon on left side is called RL, respectively (see Fig. 3).

The growth of corrosion was annually observed by the increasing of corrosion area, the increasing of corrosion length and the changing of color of metallic corrosion. In this study, each cell in each module was individually taken a high-resolution digital image in every year during the 12th–15th year of operation, then we used the ImageJ program to manipulate the calculation of corrosion area. The threshold of color or quantization levels of image were used to quantify the area of corrosion. Reference is made to the ASTM D130 standard regarding colors of corrosion products.

PV modules installed in the system were commercial modules with local assembly. By reviewing from the manufacturing process at that time, ribbons were generally used copper (Cu) coated with Tin-lead alloy (SnPb). Surface of cell busbars were silver (Ag). Soldering metal

(a) Top view of ribbon surface by light microscope

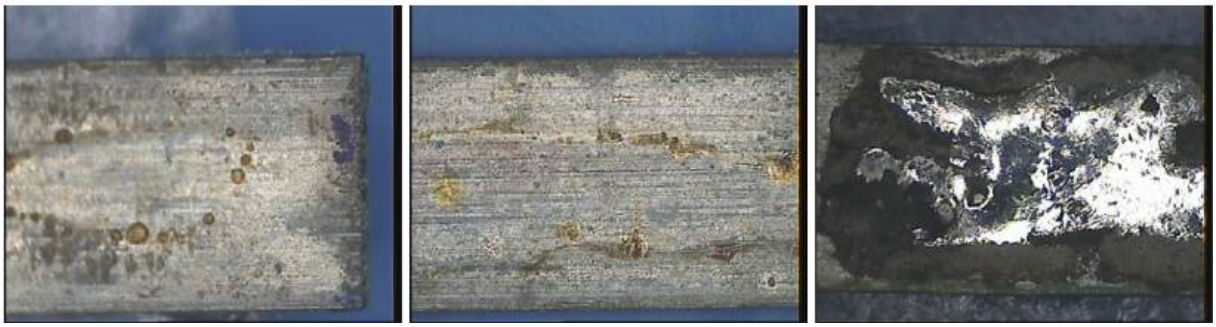

(b) Bottom view of ribbon surface by light microscope

Fig. 20. Images of ribbon surface obtained by light microscope (with ×50).

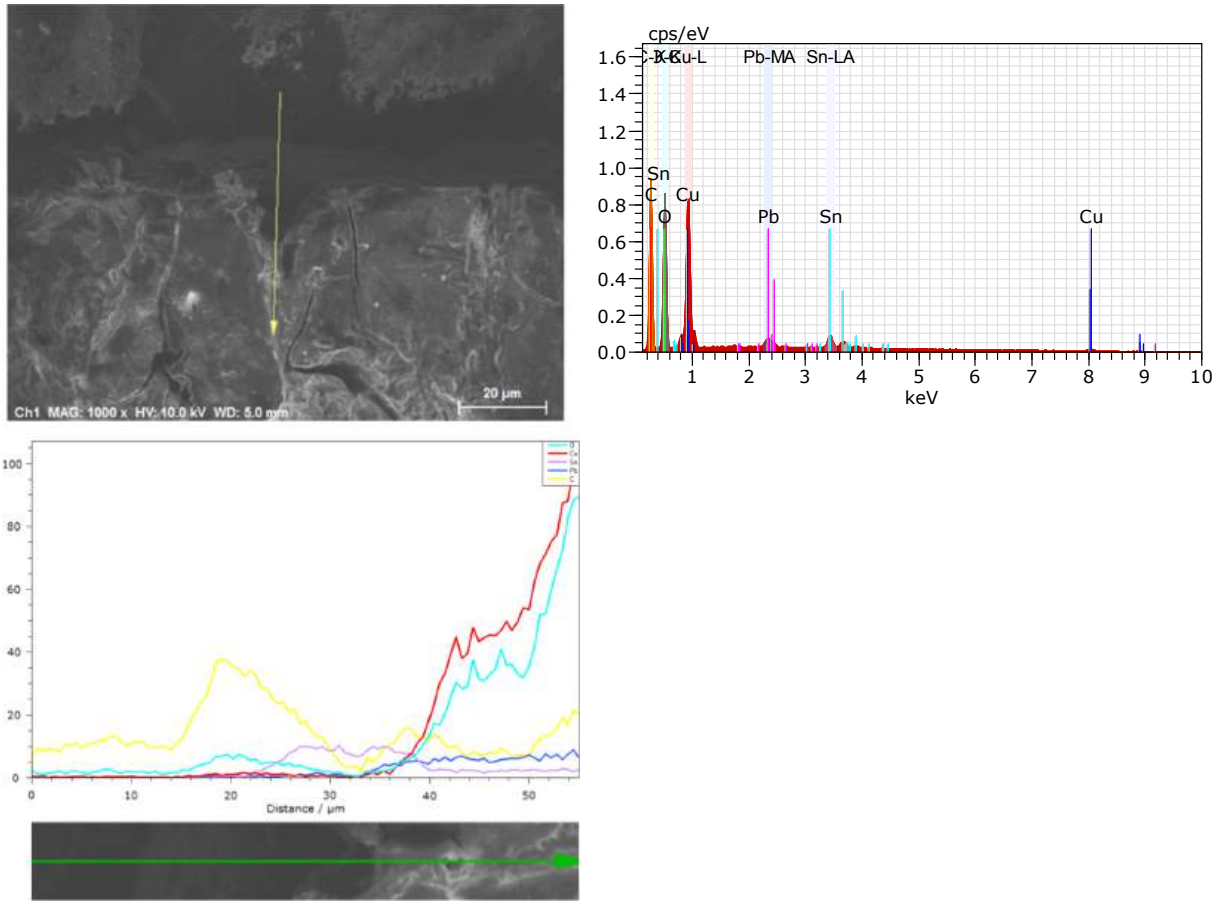

Fig. 21. SEM images and EDS line scanning of cross-section of ribbon.

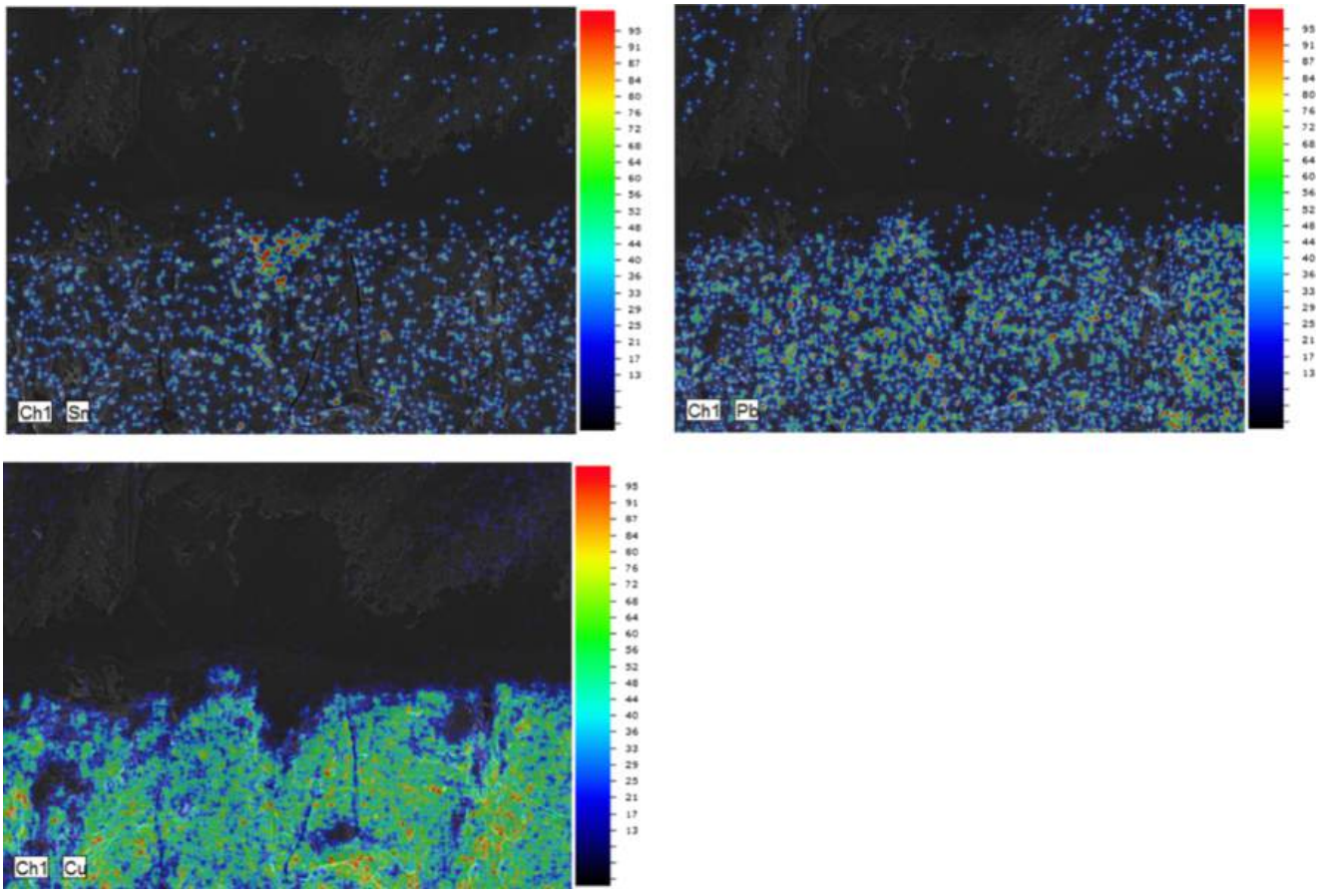

Fig. 22. EDS mapping results of ribbon cross-section.

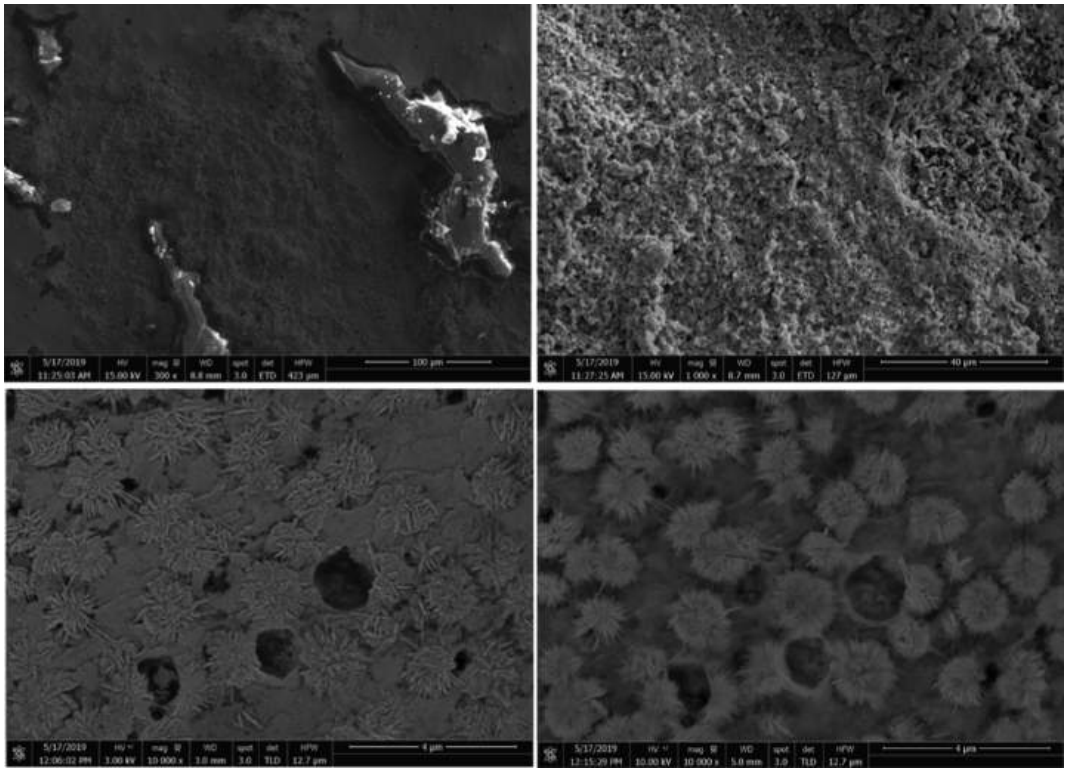

Fig. 23. SEM images of Pb corrosion product.

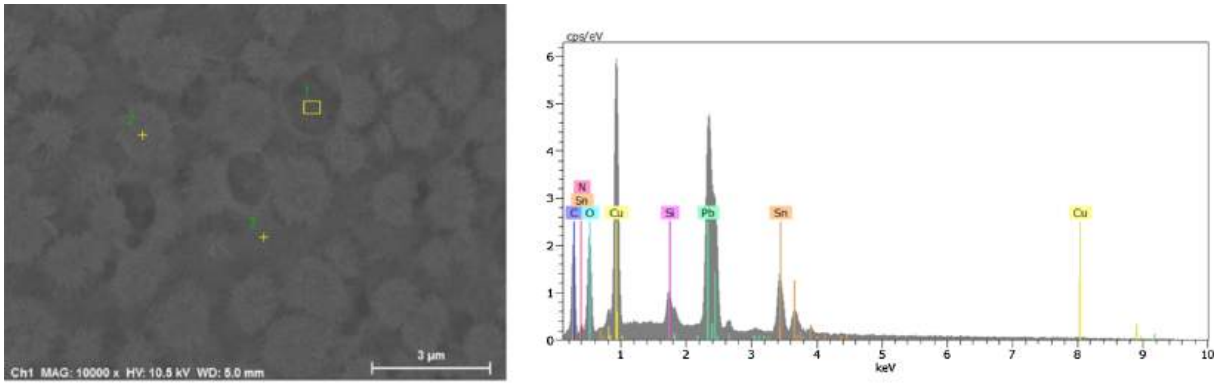

Mass percent (%)

Spectrum	C	N	O	Si	Cu	Sn	Pb
1	16.40	2.26	4.88	0.71	48.58	22.00	5.18
2	9.64	-	15.46	2.70	0.55	2.73	68.92
3	12.06	-	16.17	3.38	2.21	7.87	58.32

Fig. 24. SEM image and EDS results of Sn and Pb corrosion product.

were made of lead (Pb). The metal corrosions may simultaneously be occurred from various corrosion mechanisms. The possible corrosion products may consist of PbO, Pb(OH)2, SnO or Sn(OH)2.

For modules installed in the system in this paper, we intend to continue operation until end-of-life of the system. Therefore, these modules should not be destructed in the experiment. To understanding metal corrosion on a solar cell in-depth, we had also destructed another c-Si PV module with local assembly and with similar manner of deterioration. A number of cells, from another broken module, were taken to investigate by light microscope, Scanning Electron Microscope (SEM) and Energy Dispersive X-ray Spectrometer (EDS).

3. Results and discussion

In this study, all 16 PV modules, in one string of grid-connected system, were installed on the flat roof of a building since 2003. The tilt angle of modules was 14°and facing to the South. In-plane solar irradiation of the system were between 1843 and 2005 kWh/m^2/year. From system monitoring data during 2018–2019, the 50th percentile of in-plane daily solar irradiation was 5.21 kWh/m^2/day. The average of in-plane solar irradiation was about 1928 kWh/m^2/year. It means that all poly-Si modules in this investigation were exposed under sunlight about 28.9 MWh/m^2 for 15 consecutive years at 2018. For the weather conditions, the average ambient temperature was about 29 °C, and the average of relative humidity was about 78%RH. The values of recorded module temperature were in range of 19.6–67.4 °C.

3.1. Testing results and evaluation of PV modules

All 16 modules were annually measured in 3 test items consisting performance at standard test condition (STC), visual inspection and insulation test according to IEC61215:2005 detailed in the section 2.2. The testing results were done by the standard testing laboratory according to ISO/IEC17025 accreditation. Every year (excepted the 8th year), all modules were taken to test back and forth from the system and the laboratory since 2010 or the 7th year after operation. Firstly, electrical parameters of the current–voltage characteristics (IV characteristics) of each module were compared to its nameplate values. The comparison results are shown in Figs. A1 and A3 and in Table 4. Unfortunately, there is no standard measurement data of each module as initial values in prior to installation. It cannot be ensured the deviation of the actual measurement values and the nameplate values before operation. Therefore, the results should also be analysed by using measured results of the 7th year after operation as the base case.

The annual degradation rate of each parameter, analyzed by the results of performance at STC, can be calculated by Eq. (1) in comparison with values at the 7th year as the base case. The average values of degradation rates were shown in Fig. 4.

From the results of performance at STC measurements, it is found that

- At the 9th year: Pm of 31% of total modules were less than 90% of nameplate value.
- At the 11th year: Pm of all modules were less than 90% of nameplate value.
- At the 13th year: Pm of 13% of total modules were less than 80% of nameplate value.
- At the 15th year: Pm of 75% of total modules were less than 80% of nameplate value.

From Fig. 5(a), Pm of all modules were less than 90% of Pm at the base case during the period of 8 consecutive years (the 7th to 15th year). It means that the annual degradation of Pm of most of all modules were more than 2% after 10 years operation as shown in Fig. 5(b) and (c).

Most of manufacturers generally provide a power warranty for a period of 25 years, or some of them provide 30 years warranty. They guarantee the power output will be not less than 80% of nameplate value or the power degradation will not more than 20%. For PV power plants or large-scale solar rooftop systems, there are strong contract conditions to check and claim their products. For small systems, especially rural electrification in remote area, it is quite difficult to ensure the quality of products at the first operation and during years of operation.

In our country, there was no standard testing laboratory for PV modules testing until 2010. Hence, a standard testing laboratory was

funded by Department of Alternative Energy Development and Efficiency (DEDE), and Energy Conservation Fund in Ministry of Energy, to set up the testing facility in our university since 2006. It is essential to ensure the quality of products and consumer protection.

The annual degradation rates of electrical parameters can be calculated by Eq. (1). The evaluation is normally based on their nameplate values. In this paper, we calculated in comparison with both their nameplate values and their measured results in each year. In the period of measurement, 8 years, the 7th year to the 15th year), Pm of all modules decreased more than 10% from the base case. The annual power degradation results, based on the 7th year, were more than 2% per each year for over than 50% of total modules since the 10th year. In the 15th year, the annual power degradation results were more than 3% per year for 70% of total modules. The degradation rates of modules since the 10th year after operation were in the range of 2.5–3.0%. The distribution of population of modules can be found in Fig. 5(b) and (c).

For the insulation test according to IEC61215:2005 clause 10.3, it was found that the insulation results, in both withstand test and insulation resistance test, passed the criteria for all modules in each year.

3.2. Results of corrosion growth

The schematic and layout of modules in the string including the running code, modules and cells, used in this paper were shown and defined in Section 2.3. We selected the 5 modules from total 16 modules to demonstrate in this paper. The selected modules consist of a module located at the positive end (M1), a module located at negative end (M16), a module located at the middle of string (M8) and other two modules with maximum percentage of power degradation (M13 and M14). In this section, the selected modules were called Module A, B, C, D and E, respectively.

Images of modules, cells and electroluminescence (EL) were obtained by the visual inspection test and EL measurement come from the standard testing laboratory as well as the results in the section 3.1. There were visual images of modules since the 9th year. Images of cells were taken since the 12th year. EL images were taken since the 13th year.

The visual images, during the 9th to the 15th year, of the M13 module called Module C, were shown in Fig. 6 for example. The deterioration or defects observation on modules were focused such as in Fig. 7. Fig. 8 shows the example of visual defects observation on each cell in each module.

The deterioration on the rear side of modules can be annually observed. It is noted that the backsheet color of each module was light brown since the 9th year after operation. From images of modules at the 12th year, the backsheet delamination was observed beside their junction boxes around 20% of total module area, and the beginning of chalking of backsheet was found. The backsheet layer separation was found. From images at the 13th year, the backsheet delamination area was around 50% of total module area, and EVA appearance was especially found in the module area without cell. In the 14th and 15th year, the area of backsheet delamination was more than 80% and completely, respectively.

From the visual images on the front side of modules, the browning, crack, corrosion, delamination and snail trail on superstrate materials were appeared in all modules. On the rear side of modules, the deterioration, consisting of backsheet browning, delamination and chalking, were appeared on the substrate materials as shown in Fig. 6. In the 15th year, the backsheet delamination was presented more than 80% of total area of all modules.

There were EVA browning appearance on every cell of all modules since the 12th year. During the 12th to the 15th year, EVA browning area on each cell was not significantly changed, but the degree of browning or the light brown was slightly changed to dark brown annually. From the population of images of cells, the browning area can be classified into 3 groups consisting of (a) the browning appeared over 90% of cell area, (b) the browning appeared over 50% of cell area, and (c) the browning scattering appeared in small pieces over cell area. Fig. B1shows the three groups of browning appearance. It is found that most of cells, more than 70% of total cells of all modules, was classified in group (c). There were 20% of total cells classified in group (b), and the left 10% of total cells were in group (a). In case of group (a), there were not other defects such as ribbons or gridline corrosions. In other hands, there were other defects, such as delamination, corrosions, snail trial, on cells in group (b) and (c).

The increasing of delamination area appeared on each cell was simultaneously investigated. The details of delamination issue is going to be reported separately. Visual images of cells were taken and then processed with the ImageJ program to quantize each image into binary level as shown in Fig. B2.

In Figs. B3 and B.4, the Electroluminescence (EL) images were also taken for all modules since the 13th year. There were many types of crack cells found in M13 module. Details of crack cells were mentioned in other reports such as IEA-PVPS Task13 report (Köntges et al., 2014).

This paper focuses on the growth of metallic corrosions occurring on each cell. The five modules were selected to describe the corrosion growth in this work. A junction box of each module is located at the back side beside the two cells, C21 and C31, at the front side view. Therefore, the both cells should be highlighted for corrosion. The metallic corrosions on ribbons and gridlines consist of yellow, light gray, dark brown and black as shown in Figs. 9 and 10. Images of metallic corrosion of cell C31 of each module were compared at the 15th year. The schematic and layout of selected modules, and cell layout on each module, and Pm measured results are shown in Fig. 11. From the Pm results of selected modules, the M13 or Module C was not the lowest Pm at the 7th year (the first year of observation), but it was the lowest Pm at the 15th year with maximum degradation rate and annual Pm degradation.

The ribbon corrosion colors were yellow, brown and light gray in the 12th and 13th year, then changed to dark brown, gray and black in the 14th and 15th year as shown in Fig. 12. Hence, gridline corrosion was yellow in the 12th – 13th year, then changed to dark brown and black in the 14th and 15th year.

Fig. 13 shows the number of cells counting each corrosion color in each selected module during the 12th–15th year after the PV system operation. Total number of cells in each module is 36 cells in series. Colors of corrosion found in this study consist of yellow, gray, dark brown and black. The number of cells with corrosion in black increased in the later years.

The corrosion areas on the ribbons, of each cell of selected modules, were calculated based on total area of each ribbon. The total area of two ribbons is 6.72 cm^2. Fig. 14 describes the method how to determine the corrosion area on the ribbon of cell. The threshold of color or quantization levels of image were used to quantify the area of corrosion. Reference is made to the ASTM D130 standard regarding colors of corrosion products. The area calculation was done by the ImageJ program on each visual image of cell. The corrosion growth along the width of ribbon was limited by the width, but the growth along the length of ribbon was annually dominant on the increasing of corrosion area. The calculation of the ratio of corrosion area and total ribbon area can be shown in Fig. B5. The ribbon corrosion on C21 cells appeared only on Module B and D. While we focus on the growth of corrosion area of ribbons on C31 cell, the cell beside the junction box, of each selected module, it is found that the corrosion area, on both ribbons of

C31 cell, of Module B was larger than other selected modules. For C31 of Module B, the corrosion area increasing was 13% of total ribbons area during 4 years under observation. For the four selected modules, except Module D, the corrosion areas increased around 10 to 17% of each total ribbon area during the 12th–15th year after operation. The high steepness of corrosion growth was observed between the 12th and the 13th year after operation (see Fig. 15).

In Fig. 16, results of series resistance, Rs, of each selected module were plotted during the 12th–15th year. It cannot be summarized that the more the corrosion area, the higher the Rs. It means that the corrosion appearance on the cell ribbon may not be significant to the electrical resistance of the interconnection contacts.

When we turn back to images of rear side of the five selected modules as shown in Fig. B5, the backsheet delamination, especially near the frame edge beside the junction box, may affect to develop the growth of metal corrosion on cells.

The analysis of PV module deterioration is based on the model of causes and effects as shown in Fig. 17. This investigation emphasizes on the metallic corrosion growth on cell. Fig. 17 describes the metallic corrosion on ribbons beginning with the delamination of Ethylene Vinyl Acetate (EVA) and moisture penetration ingression into a module. The encapsulant material, EVA, delamination can be occurred by UV and Thermal impacts under field exposure. The two main products of broken EVA chemical bond consist of acetic acid and aldehyde (Xiong et al., 2017). Then, acetic acid, which oxygen rich, becomes the electrolyte of the galvanic reaction of each dissimilar bimetal couple on solar cells in modules. There are four parts, in a general galvanic corrosion cell, consisting of anode, cathode, electrolyte and electrical connection between anode and cathode. At the time of this system installation, ribbons materials were generally used copper (Cu) coated with Tin-lead alloy (SnPb), and the surface of cell busbars were silver (Ag), and soldering metal were made of lead (Pb). So, the corrosion products may possible consist of PbO, Pb(OH)2, SnO or Sn(OH)2. The standard electrode potential at 25 °C of Ag, Cu, Pb and Sn are + 0.800, +0.520, −0.125 and −0.137, respectively (see Fig. 18).

Reference is made to the ASTM standard D130, the colors of corrosion product are listed

- PbO and Pb(OH)2 appearing in blue amorphous and dark-brown or black.
- SnO2 and Sn(OH)2 appearing in yellow or light gray and white
- CuO and Cu(OH)2 appearing in black and blue green (patina)

Fig. 19 demonstrates the corrosion products and their colors for example of Module B in the 14th year after operation. From the galvanic corrosion (Xiong et al., 2017), the chemical reaction galvanic cell can be listed

Anode; $Sn \rightarrow Sn^{2+} + 2e^{-}$, $Pb \rightarrow Pb^{2+} + 2e^{-}$

Cathode; $2H_2O + 2e^{-} \rightarrow 2OH^{-} + H_2\uparrow$

In acetic acid $Sn + 2H^{+} \rightarrow Sn^{2+}2H_2\uparrow$, $Pb + 2H^{+} \rightarrow Pb^{2+} + 2H_2\uparrow$

For modules installed in the system in this paper, we intend to continue operation until end-of-life of the system. Therefore, these modules should not be destructed in the experiment. To understanding metallic corrosion on a solar cell in-depth, we had also destructed another c-Si PV module with local assembly and with similar manner of deterioration. A number of cells, from another broken module, were taken to investigate by light microscope, Scanning Electron Microscope (SEM) and Energy Dispersive X-ray Spectrometer (EDS).

The corrosion products and color of corrosion products can be justified by EDS and referred to ASTM D130 standard. From Figs. 20–24, the colors of corrosion products on ribbon surface consisted of yellow, dark-brown, light gray, and blue green (patina). Figs. 21 and 22 are to confirm Pb and Sn density decreasing and Cu remaining. Figs. 23 and 24 confirm the Sn and Pb corrosion product by SEM and EDS mapping.

4. Conclusions

The deterioration of PV modules, put into operation more than 15 consecutive years in Thailand, was focused in this investigation. One string of poly-Si PV modules, installed in a grid-connected system since 2003, were selected in this study. All 16 modules were annually taken to measure back and forth from system and in the standard testing laboratory since the 7th year after operation. From the results of performance at STC, it was found that Pm of 75% of total modules were less than 80% of the nameplate value in the 15th year. The annual power degradation results were more than 3% per year for 70% of total modules in the 15th year. The degradation rates of modules since the 10th year after operation were in the range of 2.5 to 3.0%. In this paper, the metallic corrosion growth on ribbons was highlighted. During the 12th–15th year, the corrosion area growth on cell ribbons was around 10–17% of ribbons area, especially for cells beside junction box of its module. From the Rs results, it cannot be summarized that the more the corrosion area, the higher the Rs. The colors of corrosion products were also observed in both color appearance and color change on each cell of selected modules. In this study, we found colors of corrosion products consisting of yellow, gray, dark brown and black. So, the corrosion products may possible consist of PbO, $Pb(OH)_2$, SnO or $Sn(OH)_2$. For modules installed in the system in this paper, we intend to continue operation until end-of-life of the system. Therefore, these modules should not be destructed in the experiment. To understanding metallic corrosion on a solar cell in-depth, we had also broken another c-Si PV module with local assembly and with similar manner of deterioration.

Declaration of Competing Interest

The authors declare that they have no known competing financial interests or personal relationships that could have appeared to influence the work reported in this paper.

Acknowledgements

Authors would like to thank CES Solar Cells Testing Center (CSSC), Pilot Plant Development and Training Institute of the university, ISO/IEC17025 accreditation laboratory, for supporting the testing results. The.

Joint Graduate School of Energy and Environment (JGSEE) for providing partial research grants to support this work. We are also sincerely grateful to Dr. Kobsak Sriprapha from National Science and Technology Development Agency, Dr. Napachat Tareelap from School of Energy Environment and Materials of the university , Dr.Amporn Wiengmoon and Dr. Buntoon Wiengmoo from Naresuan University for valuable comments.

Appendix A

See Figs. A1–A3.

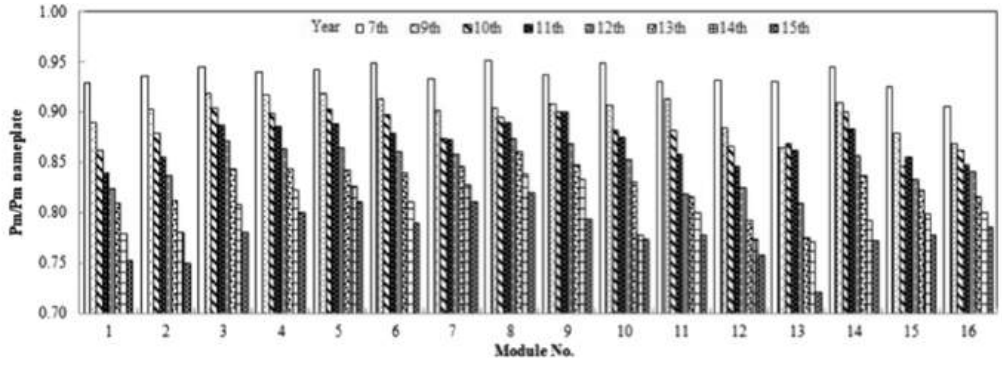

(a) Ratio of measurement values and nameplate values of Pm from the 7th to the 15th year each module

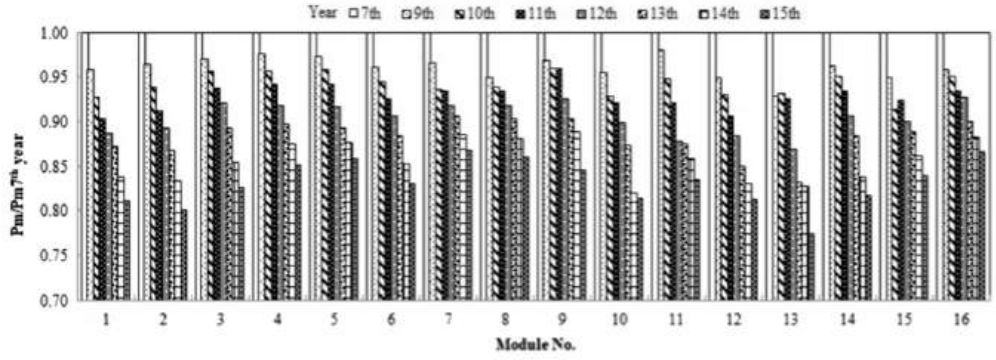

(b) Ratio of measurement Pm and Pm at the base case (the 7th year) of 16 modules

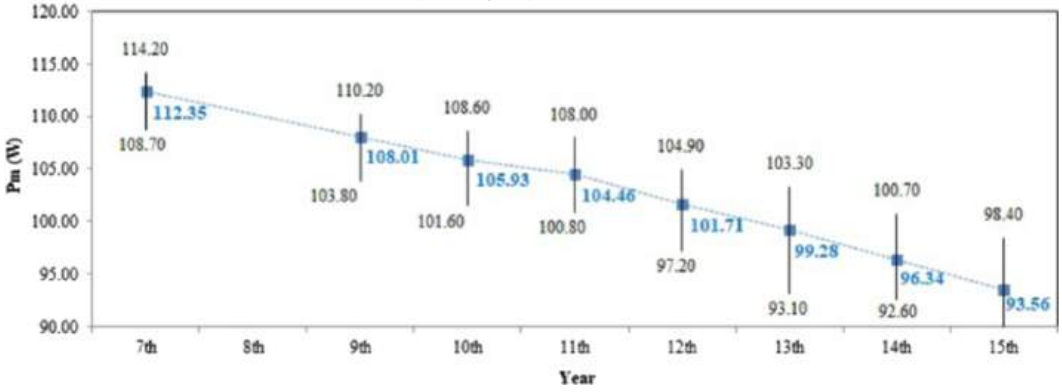

(c) The average, maximum and minimum of Pm from 16 modules in each year.

Fig. A1. Measurement values of Pm from the 7th to the 15th year.

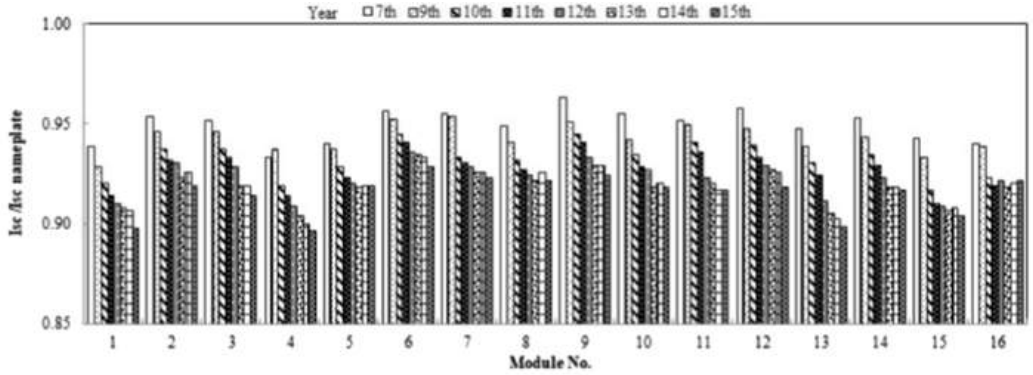

(a) Ratio of measurement values and nameplate values of Isc from the 7th to 15th year of 16 modules

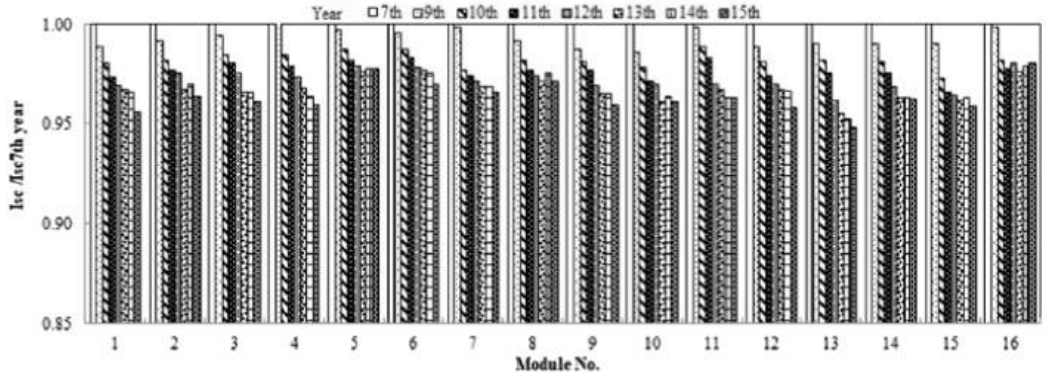

(b) Ratio of measurement Isc and Isc at the base case (the 7th year) of 16 modules

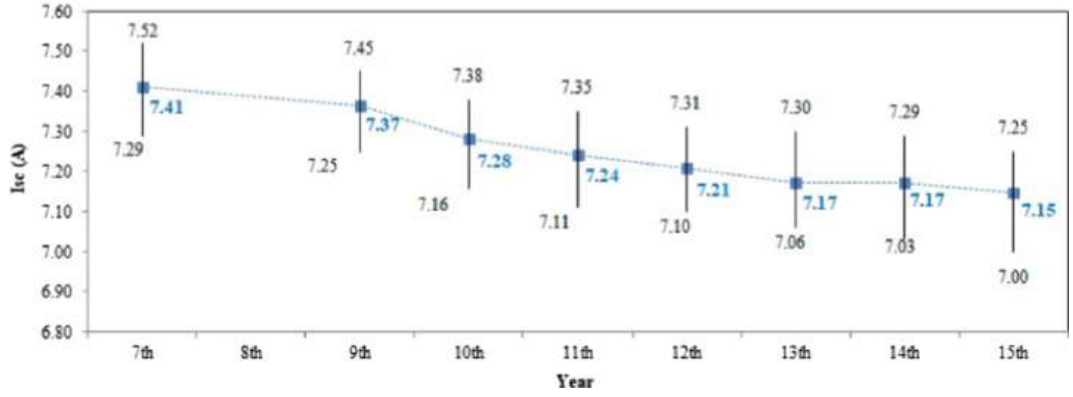

(c) The average, maximum and minimum of Isc from 16 modules in each year.

Fig. A2. Measurement values of Isc from the 7th to the 15th year.

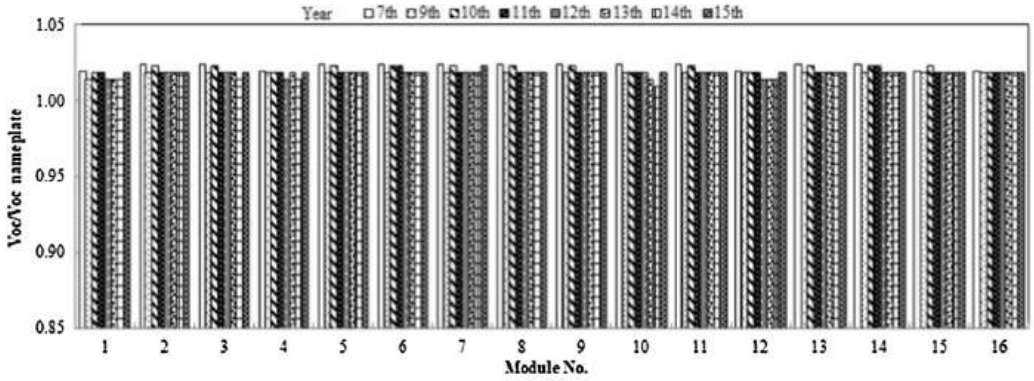

(a) Ratio of measured values and nameplate values of Voc from the 7th to the 15th year of 16 modules

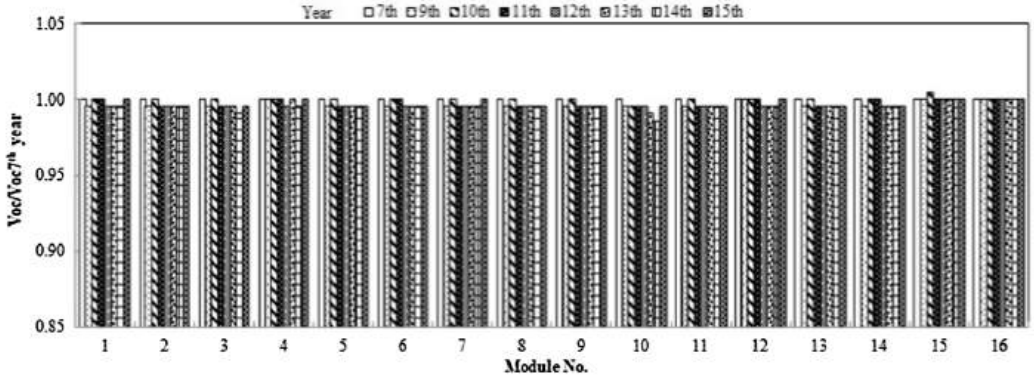

(b) Ratio of measured Voc and Voc at the base case (the 7th year) of 16 modules

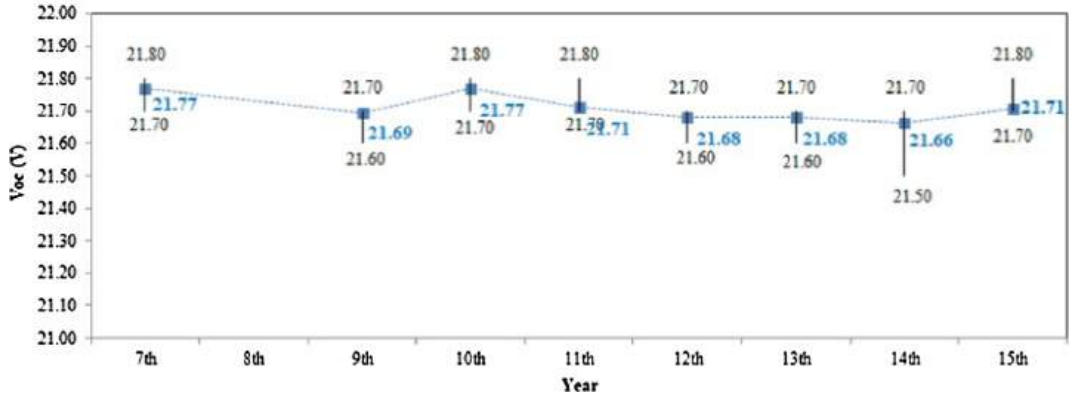

(c) The average, maximum and minimum of Voc from 16 modules in each year.

Fig. A3. Measurement values of Voc from the 7th to the 15th year.

Appendix B

See Figs. B1–B5.

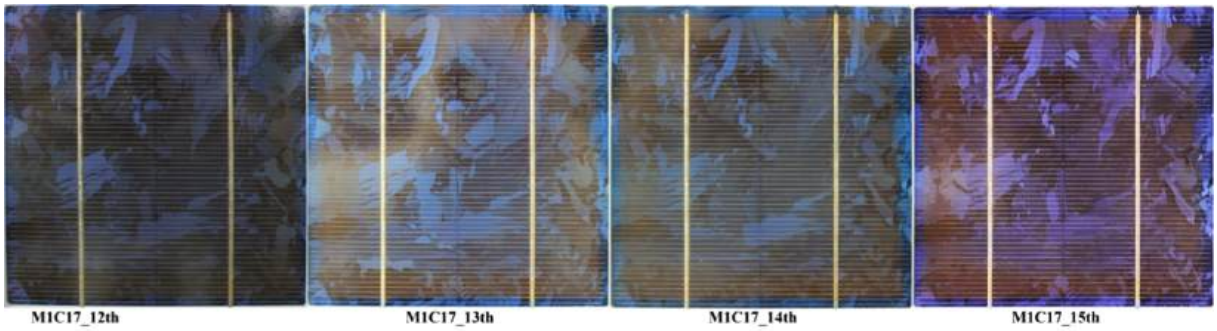

(a) the browning appeared over 90% of cell area

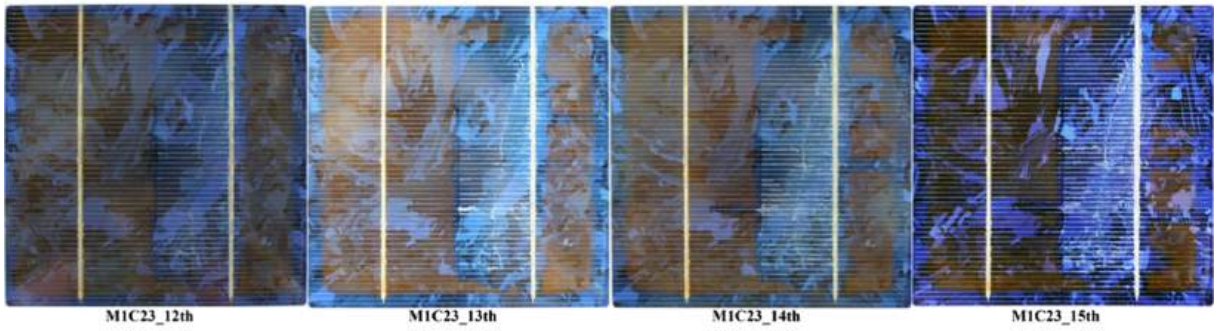

(b) the browning appeared over 50% of cell area

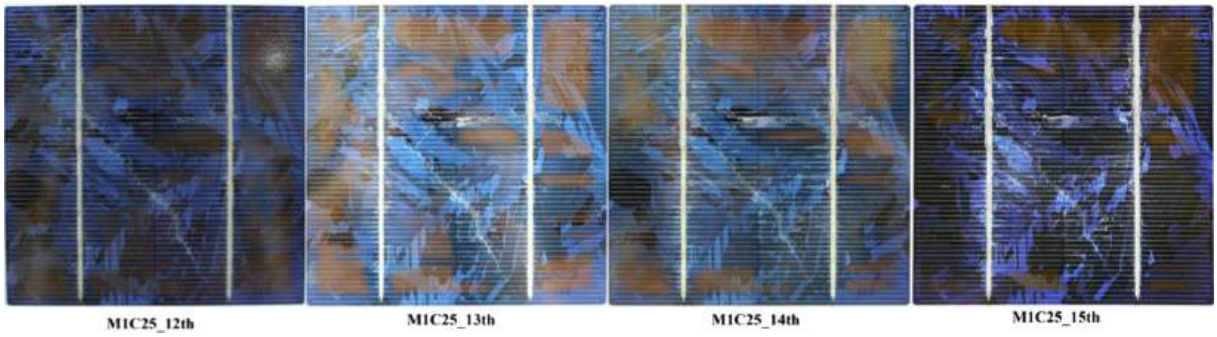

(c) the browning scattering appeared in small pieces over cell area

Fig. B1. Browning appearance on cells can be classified into 3 groups (a) the browning appeared over 90% of cell area, (b) the browning appeared over 50% of cell area, and (c) the browning scattering appeared in small pieces over cell area.

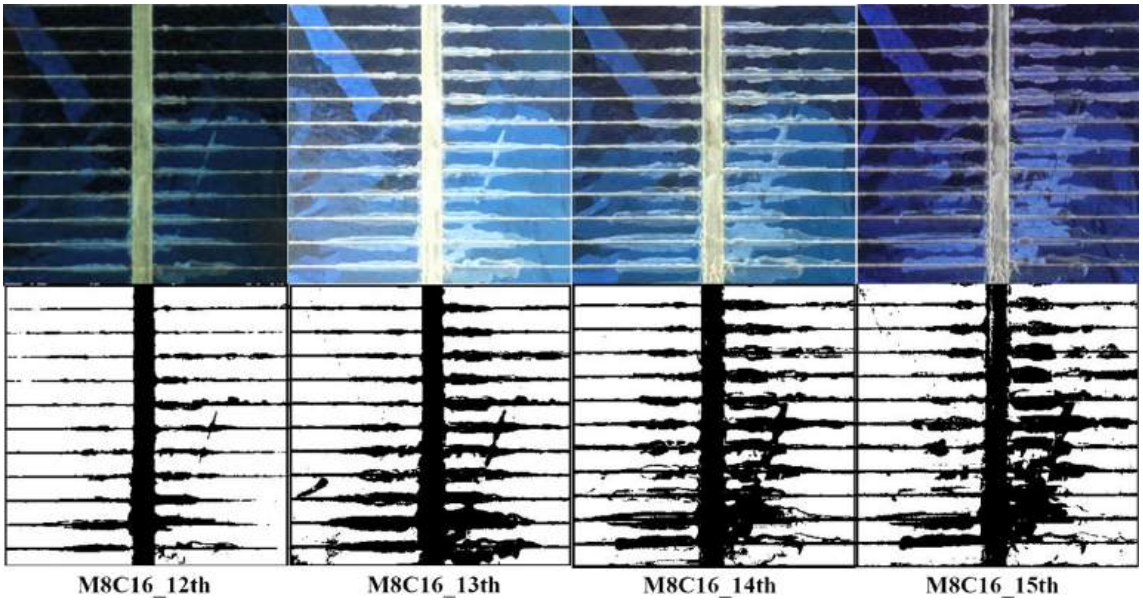

Fig. B2. Increasing of delamination areas on a part of cell in cell No.16 on the M8 module.

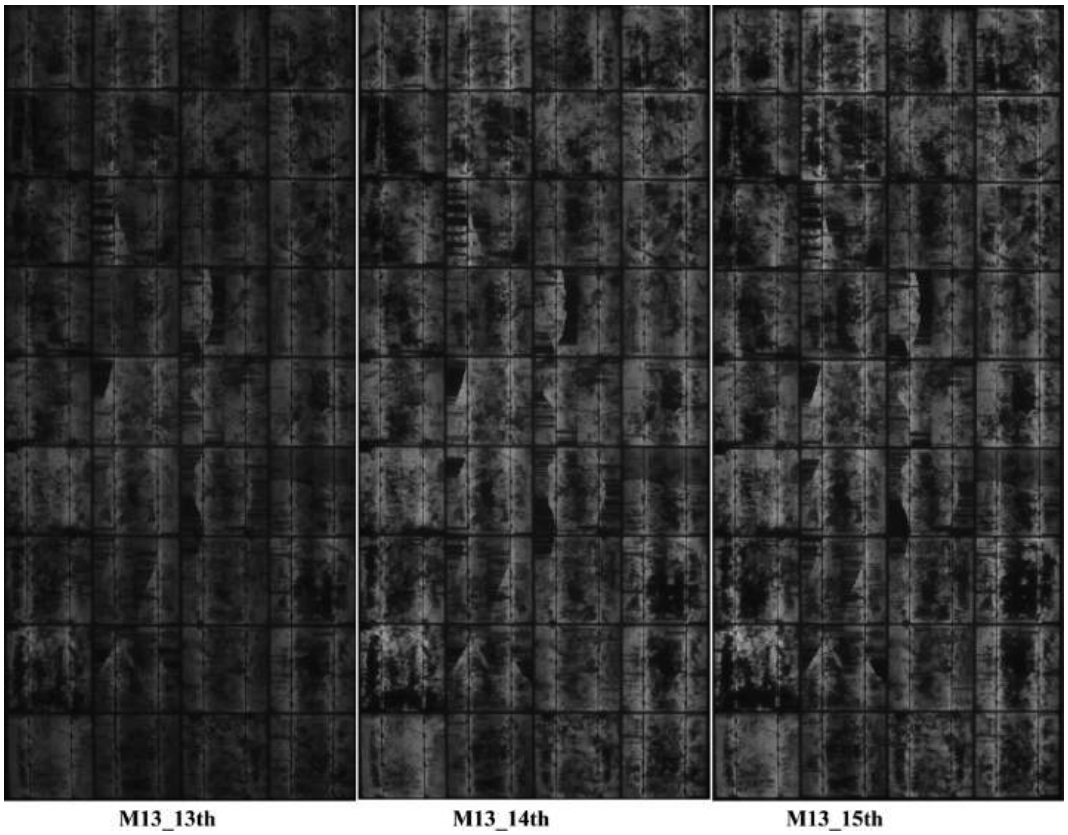

Fig. B3. EL images of M13 module during the 13th to the 15th year.

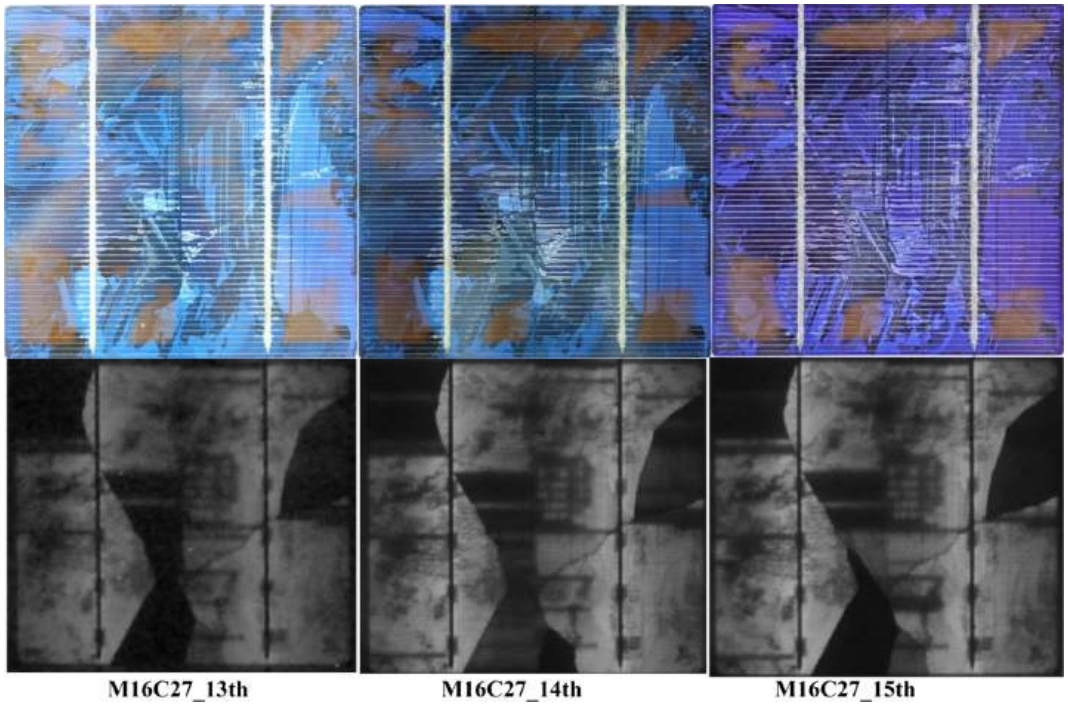

Fig. B4. EL images of cells in M16 module during the 13th to the15th year.

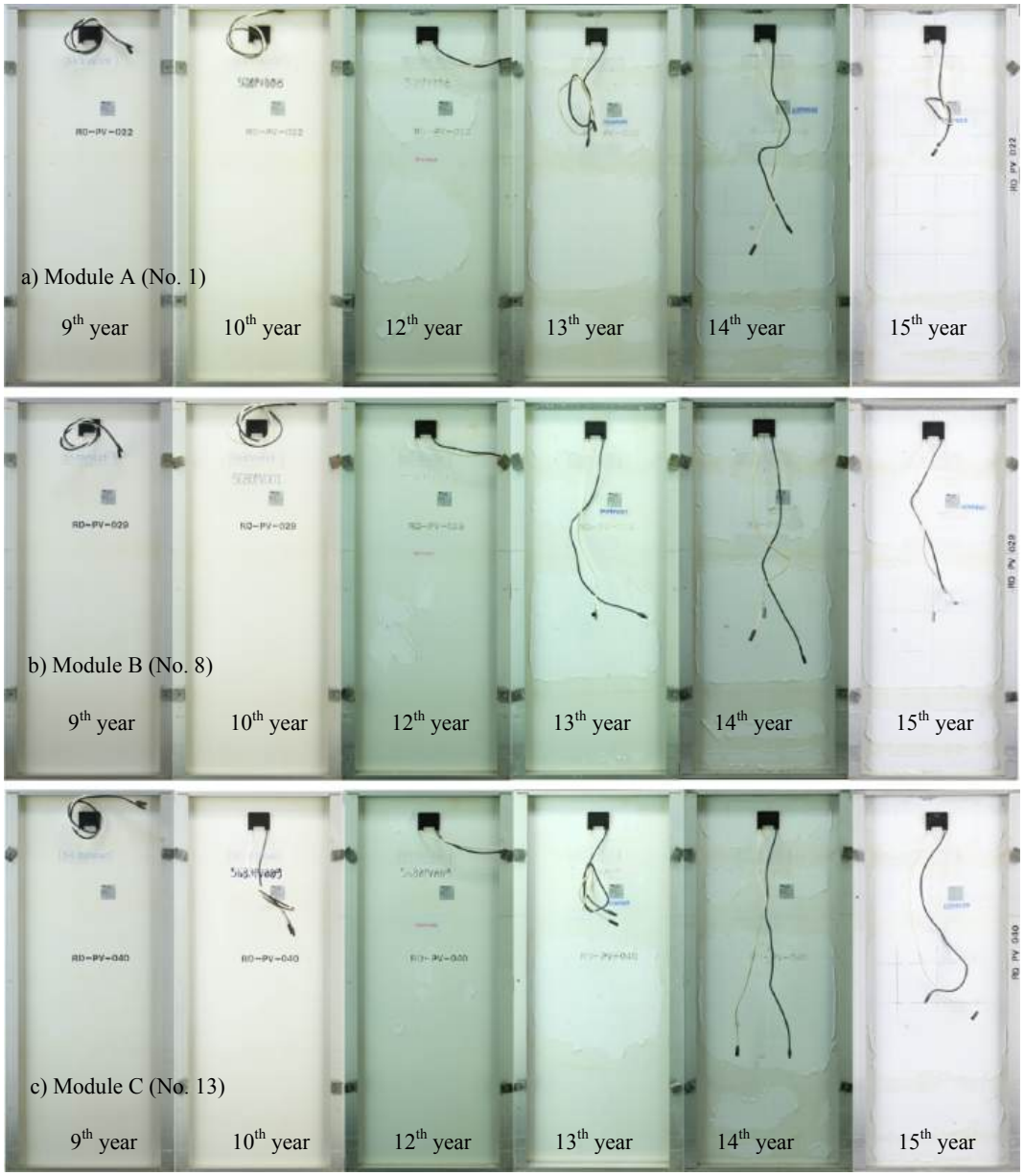

Fig. B5. Images of rear side of the 5 selected modules.

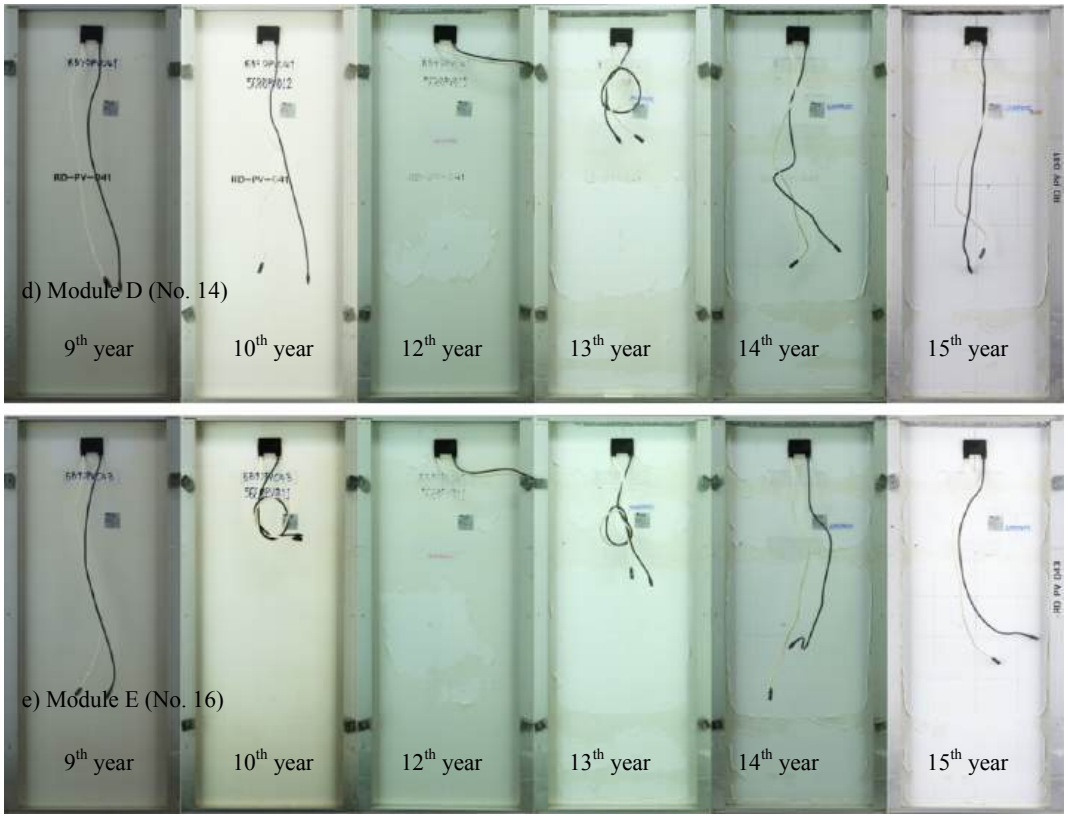

Fig. B5. (*continued*)

References

BBW, 2003. Mean Time Before Failure of Photovoltaic modules. SUPSI, DACD, LEEE-TISO.

DEDE, 2019. Thailand PV status report 2018. Department of Alternative Energy Development and Efficiency, Ministry of Energy, Thialand.

da Fonseca, J.E.F., de Oliveira, F.S., Massen Prieb, C.W., Krenzinger, A., 2020. Degradation analysis of a photovoltaic generator after operating for 15 years in southern Brazil. Sol. Energy 196, 196–206.

Ferrara, C., Philipp, D., 2012. Why do PV modules fail? Energy Procedia 15, 379–387.

Gagliardi, M., Lenarda, P., Paggi, M., 2017. A reaction-diffusion formulation to simulate EVA polymer degradation in environmental and accelerated ageing conditions. Sol. Energy Mater. Sol. Cells 164, 93–106.

IEA-PVPS, 2009. Trends in photovoltaic applications survey report of selected IEA countries between 1992 and 2008. Report No. IEA-PVPS T1-18.

Ishii, T., Masuda, A., 2017. Annual degradation rates of recent crystalline silicon photovoltaic modules. Progr. Photovolt. Res. Appl. 25, 953–967.

Janakeeraman, S.V., Singh, J., Kuitche, J., Mallineni, J.K., TamizhMani, G., 2014. A statistical analysis on the cell parameters responsible for power degradation of fielded pv modules in a hot-dry climate. In: 2014 IEEE 40th Photovoltaic Specialist Conference (PVSC). pp. 3234–3238.

Jordan, D.C., Kurtz, S.R., 2013. Photovoltaic degradation rates-an analytical review. Progr. Photovolt. Res. Appl. 21 (1), 1–32.

Jorgensen, G.J., Terwilliger, K.M., DelCueto, J.A., Glick, S.H., Kempe, M.D., Pankow, J.W., Pern, F.J., McMahon, T.J., 2006. Moisture transport, adhesion, and corrosion protection of PV module packaging materials. Sol. Energy Mater. Sol. Cells 90 (16), 2739–2775.

Kraft, A., Labusch, L., Ensslen, T., Dürr, I., Bartsch, J., Glatthaar, M., Glunz, S., Reinecke, H., 2015. Investigation of acetic acid corrosion impact on printed solar cell contacts. IEEE J. Photovolt.. 5 (3), 736–743.

Kim, N., Lee, S., Zhao, X.G., Kim, D., Oh, C., Kang, H., 2016. Reflection and durability study of different types of backsheets and their impact on c-Si PV module performance. Sol. Energy Mater. Sol. Cells 146 (Supplement C), 91–98.

Li, J., Shen, Y.-C., Hacke, P., Kempe, M., 2018. Electrochemical mechanisms of leakage-current-enhanced delamination and corrosion in Si photovoltaic modules. Sol. Energy Mater. Sol. Cells 188, 273–279.

Limmanee, A., Udomdachanut, N., Songtrai, S., Kaewniyompanit, S., Sato, Y., Nakaishi, M., Kittisontirak, S., Sriprapha, K., Sakamoto, Y., 2016. Field performance and degradation rates of different types of photovoltaic modules: A case study in Thailand. Renew. Energy 89 (Supplement C), 12–17.

(Mani) GovindaSamy TamizhMani, J.K., 2013. Accelerated Lifetime Testing of Photovoltaic Modules. Solar America Board for Codes and Standards Report, pp. 1–106.

Masson, G.K., Izumi, 2019. Trends 2019 in photovoltaic applications: IEA-PVPS Task 1: Strategic PV Analysis and Outreach. International Energy Agency, Photovoltaic Power Systems Programme (IEA-PVPS).

Masson, G.K., Izumi, Detollenaere, A., Lindahl, J., 2019. 2019 Snapshot of Global PV Markets: IEA-PVPS Task 1: Strategic PV Analysis and Outreach. International Energy Agency, Photovoltaic Power Systems Programme (IEA-PVPS).

Köntges, M., Kurtz, S., Packard, C., Jahn, U., Berger, K., et al., 2014. IEA PVPS T13-01; Review of failures of photovoltaic modules. In: Systems, P.a.R.o.P. (Ed.) Review of Failures of Photovoltaic Modules. International Energy Agency Photovoltaic Power Systems Programme, pp. 1–140.

Rajput, P., Tiwari, G.N., Sastry, O.S., Bora, B., Sharma, V., 2016. Degradation of monocrystalline photovoltaic modules after 22years of outdoor exposure in the composite climate of India. Sol. Energy 135, 786–795.

Sangpongsanont, Y., Chenvidhya, D., Chuangchote, S., Limsakul, C., Seapan, M., Muenpinij, B., Chenvidhya, T., Jivacate, C., Kirtikara, K., 2013. Long-term monitoring of a small residential rooftop PV gird-connected system in Thailand. In: 23th International Photovoltaic Science and Engineering Conference (PVSEC-23). Taipei, Taiwan.

Sangpongsanont, Y., Chenvidhya, D., Chuangchote, S., Limsakul, C., Seapan, M., Muenpinij, B., Chenvidhya, T., Parinya, P., Kirtikara, K., 2016. Thirteen-year Long-term Monitoring and Reliability of PV Module Degradation in Thailand. In: 26th International Photovoltaic Science and Engineering Conference (PVSEC-26). Singapore.

Virtuani, A., Caccivio, M., Annigoni, E., Friesen, G., Chianese, D., Ballif, C., Sample, T., 2019. 35 years of photovoltaics: Analysis of the TISO-10-kW solar plant, lessons learnt in safety and performance-Part 1. Progr. Photovolt.: Res. Appl.

Xiong, H., Gan, C., Yang, X., Hu, Z., Niu, H., Li, J., Si, J., Xing, P., Luo, X., 2017. Corrosion behavior of crystalline silicon solar cells. Microelectron. Reliab. 70, 49–58.